

ACTIVATION OF HYDROGEN PEROXIDE FOR OXIDATIONS
BY TRANSITION METAL COMPLEXES

By

MICHAEL H. ROBBINS

A DISSERTATION PRESENTED TO THE GRADUATE SCHOOL OF THE
UNIVERSITY OF FLORIDA IN PARTIAL FULFILLMENT OF THE
REQUIREMENTS FOR THE DEGREE OF DOCTOR OF PHILOSOPHY

UNIVERSITY OF FLORIDA

1995

To my parents for all their help and support over the years, and to my friends who have made my stay in Gainesville so enjoyable.

ACKNOWLEDGMENTS

I would like to thank all of those who have made my last four and a half years both enjoyable and stimulating. In particular I would like to thank Dr. Russell Drago, my advisor. If I had to choose a graduate school and research group all over again, I would still make the same choice. His wife Ruth Drago also deserves kudos for her hospitality and great home cooking at various Drago group gatherings. Many thanks are also due to the members my supervisory committee, for their patience and their time.

The members of the Drago group, past and present, deserve thanks for their help and harassment over the years. In particular, I would like to thank the current members of the oxidation subgroup: Ken (just extract it) Lo, Mike (oxygen enriched) Gonzalez, Churchill (but it's not toxic) Grimes, Alfredo (high tide) Mateus, Silvia Dias, and "Tiger" Cheng. While many other group members have helped me out over the years, having an bright group of individuals to bounce ideas off in subgroup over the last two years has been invaluable.

In addition I would like to thank the people who really get things done here at the University of Florida, the secretaries. Between Maribel Lisk and Donna Balkcom I always knew that even if I had no idea where I was supposed to be, someone I could ask did.

TABLE OF CONTENTS

ACKNOWLEDGMENTS	iii
LIST OF TABLES	vi
LIST OF FIGURES	vii
ABSTRACT	x
CHAPTERS	
1 INTRODUCTION TO PEROXIDE ACTIVATION	1
Overview of Homogeneous Catalytic Oxidation	1
Peroxide Activation	6
2 PEROXIDE ACTIVATION WITH A STERICALLY HINDERED RUTHENIUM COMPLEX	8
Introduction	8
Experimental	11
Experimental Results	14
Discussion	22
Conclusion	39
3 ACTIVATION OF HYDROGEN PEROXIDE FOR OXIDATION WITH COPPER(II) COMPLEXES	41
Introduction	41
Experimental	43
Results And Discussion	47
Conclusion	75
4 ACTIVATION OF HYDROGEN PEROXIDE FOR OXIDATION WITH VANADIUM-PEROXO COMPLEXES ...	78
Introduction	78
Experimental	82

	Results And Discussion	87
	Conclusion	94
5	CONCLUSION	96
	REFERENCES	98
	BIOGRAPHICAL SKETCH	104

LIST OF TABLES

<u>Table</u>	<u>page</u>
2-1 The $E_{1/2}$ values for the ruthenium complex at different pH levels. These values have been adjusted to reflect voltages vs. SHE	17
2-2 Initial rates for the oxidation of the ruthenium complex by hydrogen peroxide	23
3-1 Dependence of quinaldine blue oxidation rate on peroxide, $\text{Cu}(\text{PA})^+$ concentration, and substrate concentration	51
3-2 Rate of quinaldine blue oxidation for copper(II) complexes of anionic bidentate (runs 1-10) and anionic tridentate (runs 11-14) ligands	54
3-3 Rate of quinaldine blue oxidation for copper(II) complexes of neutral bidentate (runs 1-10) and neutral multidentate (runs 11-16) ligands	56
3-4 Rate of oxidation of quinaldine blue for various concentrations of copper(II) complexes of LEU and AcAc. Peroxide concentration was held constant at $2.8 \times 10^{-2} \text{ M}$	59
3-5 Rate of quinaldine blue oxidation for various peroxide concentrations with $2.8 \times 10^{-6} \text{ M}$ copper(II)-BPA (runs 1-4), $2.8 \times 10^{-5} \text{ M}$ copper(II)-AcAc (runs 5-10), and $2.8 \times 10^{-5} \text{ M}$ copper(II)-TMED (runs 11-21)	60
3-6 Values for K_m and V_{\max} as determined for the copper(II) complexes of various ligands	74
4-1 Conversion and efficiency for oxidation of cyclohexane to cyclohexanol and cyclohexanone with vanadium catalysts	92
4-2 Conversion and efficiency for oxidation of benzene to phenol with vanadium catalysts	92

LIST OF FIGURES

<u>Figure</u>	<u>page</u>
2-1 A typical cyclic voltammagram, the one shown here is for the $[\text{Ru}(\text{DMP})_2(\text{H}_2\text{O})_2]^{2+}$ complex at pH = 9.90. The scale shown is for potential vs. the Ag/AgCl reference	16
2-2 The titration curve for the ruthenium complex. Note the inflection points of the curve. Analysis of these inflections gives pKa values for the coordinated water as 3.28 and 5.13	19
2-3 A typical UV-Vis kinetic run for the oxidation of the ruthenium complex by hydrogen peroxide. The ruthenium complex absorbance at 495 nm is measured as a function of time after the addition of hydrogen peroxide to the cell	21
2-4 A comparison of the kinetic curves for the ruthenium oxidation with changes in pH. Note the similarity of initial rates, and the inability of the peroxide to completely oxidize the complex as higher pH values	24
2-5 The pH dependence of the half-reaction potentials for the reduction (A) and the oxidation (B) of hydrogen peroxide	28
2-6 A comparison of the ruthenium reduction potentials (solid lines) and the potentials for the oxidation and reduction of hydrogen peroxide (dashed lines)	32
2-7 A comparison of the reduction potentials for the methane/ methanol and peroxide/ dioxygen half-reactions	36
2-8 An alternative mechanism for oxidation of alkanes and alkenes with the $[\text{Ru}(\text{DMP})_2(\text{H}_2\text{O})_2]^{2+}$ complex in the presence of O_2 and H_2O_2	40
3-1 Oxidation of quinaldine blue with hydrogen peroxide catalyzed by copper(II) chloride + picolinic acid. $[\text{H}_2\text{O}_2] = 2.9 \times 10^{-3} \text{ M}$, $[\text{CuCl}_2] = 2.9 \times 10^{-5} \text{ M}$	48

Figure	page
3-2 The effect of ligand:metal ratio on the rate of quinaldine blue oxidation. $[\text{Cu}^{2+}] = 2.9 \times 10^{-5} \text{ M}$, $[\text{H}_2\text{O}_2] = 5.7 \times 10^{-3} \text{ M}$. All rates are expressed in terms of (moles quinaldine blue)(liter) ⁻¹ (second) ⁻¹	49
3-3 The effect of pH on the rate of quinaldine blue oxidation. The catalyst concentration used is $2.9 \times 10^{-5} \text{ M Cu}^{2+} / \text{PA}$, the peroxide concentration is $5.7 \times 10^{-3} \text{ M}$. All rates are expressed in terms of (moles quinaldine blue)(liter) ⁻¹ (second) ⁻¹	52
3-4 The proposed mechanism for oxidations with copper(II) complexes. L = ligand	62
3-5 Proposed structures for: a) the μ^2 bound peroxide and b) the hydrogen-bond stabilized copper-hydroperoxide complex.	67
3-6 The rate of oxidation as a function of peroxide concentration for the copper(II) complexes of AcAc, TMED, and BPA	70
3-7 Lineweaver-Burk plot of 1/rate vs. $1/[\text{HO}_2^-]$ for the copper-AcAc complex	71
3-8 Lineweaver-Burk plot of 1/rate vs. $1/[\text{HO}_2^-]$ for the copper-TMED complex	72
3-9 Lineweaver-Burk plot of 1/rate vs. $1/[\text{HO}_2^-]$ for the copper-BPA complex	73
4-1 Formation of the metal-peroxo complex	80
4-2 Generation of the active radical species from the vanadium peroxo complexes. (a) is for the mechanism proposed by Mimoun, (b) is for the mechanism proposed by Di Furia	80
4-3 ¹ H NMR of $\text{K}[\text{VO}_2(\text{dipic})]$. The peaks are at 8.2 (d, 2H) and 8.35 (t, 1H)	84
4-4: ¹ H NMR of $[\text{VO}(\text{O}_2)(\text{pic})(\text{H}_2\text{O})_2]$. The peaks are at 7.9 (m, 1H), 8.1 (m, 1H), 8.3 (m, 1H), and 9.5 (s, 1H)	85

4-5	Oxidation of cyclohexane catalyzed by the $\text{VO}(\text{AcAc})_2$ complex at 50°C . $[\text{C}_6\text{H}_{12}] = 0.046 \text{ M}$, $[\text{H}_2\text{O}_2] = 0.050 \text{ M}$, $[\text{VO}(\text{AcAc})_2] = 1.0 \times 10^{-4} \text{ M}$	88
4-6	Oxidation of cyclohexane catalyzed by the $\text{VO}(\text{O}_2)(\text{bipy})_2$ complex at 50°C . $[\text{C}_6\text{H}_{12}] = 0.046 \text{ M}$, $[\text{H}_2\text{O}_2] = 0.050 \text{ M}$, $[\text{VO}(\text{O}_2)(\text{bipy})_2] = 1.0 \times 10^{-4} \text{ M}$	89
4-7	Oxidation of cyclohexane catalyzed by the $\text{VO}(\text{O}_2)(\text{pic})(\text{H}_2\text{O})_2$ complex at 50°C . $[\text{C}_6\text{H}_{12}] = 0.046 \text{ M}$, $[\text{H}_2\text{O}_2] = 0.050 \text{ M}$, $[\text{VO}(\text{O}_2)(\text{pic})(\text{H}_2\text{O})_2] = 1.0 \times 10^{-4} \text{ M}$	90
4-8	Oxidation of benzene to phenol catalyzed by vanadium complexes $[\text{H}_2\text{O}_2] = 0.050 \text{ M}$, $[\text{C}_6\text{H}_6] = 0.056$, $[\text{catalyst}] = 3.0 \times 10^{-5} \text{ M}$. This reaction was carried out at 70°C	93

Abstract Of Dissertation Presented to the Graduate School of the
University of Florida in Partial Fulfillment of the Requirements
for the Degree of Doctor of Philosophy

ACTIVATION OF HYDROGEN PEROXIDE FOR OXIDATIONS
BY TRANSITION METAL COMPLEXES

By

Michael H. Robbins

May, 1995

Chairman: Russell S. Drago
Major Department: Chemistry

This dissertation examines the activation of hydrogen peroxide with transition metal complexes. The reaction of hydrogen peroxide with a ruthenium complex, $[\text{Ru}(\text{DMP})_2(\text{H}_2\text{O})_2](\text{PF}_6)_2$, was studied. The rate law for the reaction with hydrogen peroxide was determined to be first order in peroxide and ruthenium, with a rate constant of $0.3 \text{ L} \cdot \text{mol}^{-1} \cdot \text{sec}^{-1}$. The pKa values for the two waters coordinated to ruthenium were determined to be 3.28 and 5.13 through titration. An electrochemical study was performed, and based upon the high reduction potential for the VI/IV couple, modifications to the previously reported mechanism for oxidation with this complex are suggested.

The activation of peroxide by a series of copper(II) complexes in basic aqueous solutions is also examined. Copper(II) complexes of the general formula $[LCu(H_2O)_4]^{n+}$ (where L is a bidentate ligand and $n = 1$ or 2) activate hydrogen peroxide for oxidation. The copper(II) complexes of tri- and tetra-dentate ligands are shown to be inactive, as are the *bis*- complexes of bidentate ligands. The proposed mechanism for peroxide activation involves the formation of a copper(II)-hydroperoxide complex, which then rapidly oxidizes the substrate. Comparison of reaction rates with different ligand systems, and different ligand to metal ratios, lead to the conclusion that two equatorial coordination positions must be occupied by easily displaced water to form the active complex. Rate studies give an experimental rate law which is first-order in copper(II) complex, zero-order in substrate, and variable order in peroxide. The variable order in peroxide can be explained in terms of Michaelis-Menten type kinetics.

Lastly, the activation of peroxide for the oxidation of benzene and cyclohexane by a series of vanadium complexes was studied. An examination of proposed mechanisms in the literature suggested that a vanadium peroxo complex with stronger O-O bonds (in the bound peroxo) should be more active. A complex which was previously shown to have an unusually short O-O bond length was synthesized, and its reactivity studied. The results showed that, for peroxide activation, the O-O bond length did not have a significant effect on reaction rates.

CHAPTER 1 INTRODUCTION TO PEROXIDE ACTIVATION

Overview of Homogeneous Catalytic Oxidation

The purpose of this introduction is to give the reader an overview of where peroxide activation fits into the area of homogeneous catalytic oxidation. A catalyst for oxidation of organic substrates facilitates the reaction of dioxygen or hydrogen peroxide with the substrate to be oxidized. In general, the direct reaction of the substrate with dioxygen or hydrogen peroxide is very slow. The addition of a catalyst increases the rate of the oxidation by transforming the oxidant into a more reactive form.

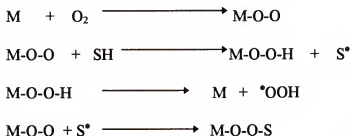
A general classification scheme for homogeneous oxidation catalysts was developed by Drago.^{1,2} This scheme divides the transition metal catalysts into five groups, each defined by the interaction between the dioxygen (or hydrogen peroxide) with the transition metal center. These five classes are

- (1) Metal bound dioxygen
- (2) Metal oxo via dioxygen
- (3) Metal oxo via peroxides
- (4) Metal peroxo systems
- (5) Metal centered oxidizing agents

Typical reactions involved in each of these five classes are summarized below. As these classes are generalized for any transition metal, the reactions are written so that the metal complex is represented by "M".

Class I: Metal Bound Dioxygen

In a Class I mechanism the dioxygen coordinates directly to the transition metal. The interaction between the metal and the bound dioxygen can be explained using the spin-pairing model of developed by Drago and co-workers.³⁻⁵ The binding of the dioxygen to the transition metal center transforms it by increasing its basicity⁶ and radical reactivity,⁷ making it able to react with a limited number of organic compounds. The reactions involved in this reaction type are shown below, where "S" is an organic substrate to be oxidized.



The M-O-O-S then decomposes to form the products via a Class IV pathway (see below). Alternate paths involve the substrate radical reacting with O₂ to generate alkyl peroxy radicals, which can then react with S-H to generate an alkyl hydroperoxide. This can then also decompose through a Class IV reaction. There are restrictions on the types of substrates which will be oxidized in this manner. The O-H bond energy for the M-O-O-H must be greater than the S-H bond energy. This limits the usefulness of Class I mechanisms, as there are few substrates where the S-H bond energy is low enough for

significant oxidation to occur. Substituted phenols are one of the few substrates observed to react with cobalt-dioxygen complexes through this mechanism.

Class II: Metal-Oxo via Dioxygen

In the Class II mechanism a high-valent metal-oxo complex is formed from the reaction of the transition metal center with dioxygen. Two ways in which this can occur have been proposed. The first is through the reaction of a metal-dioxygen complex with another metal center to form a dioxygen-bridged metal dimer. The dimer then cleaves to form high-valent metal-oxo complexes, which are the active oxidants in the system.



Another route to metal-oxo complexes with dioxygen is through a two-proton, two-electron transfer from a metal-aquo species. Dioxygen is reduced to water in the process of accepting two electrons from the metal center. The reactions involved are shown below as half-reactions.



In the Class II mechanism, the metal-oxo species is the active oxidant. The oxidation generally occurs through an oxygen atom transfer from the metal-oxo complex to the substrate.⁸

Class III: Metal-Oxo via Hydrogen Peroxide

In the Class III mechanism, the oxygen source used is hydrogen peroxide, which can also be generated in situ by the reaction with dioxygen and a sacrificial reductant. In the reaction with a transition metal complex, either a two-proton, two-electron transfer or an oxygen atom transfer occurs between the metal center and the hydrogen peroxide. The resultant high-valent metal-oxo species, which is kinetically much more reactive than hydrogen peroxide alone, will then oxidize the substrate.



Class IV: Metal Peroxo Systems

Class IV covers the majority of reactions involving a metal center and peroxides. This Class is divided up into two subclasses. In Class IVa, a transition metal complex acts as a catalyst for peroxide decomposition, and in Class IVb a metal bound peroxo species is formed from the reaction of the transition metal with hydrogen peroxide or an alkyl hydroperoxide. Both of these reactions are shown below.

Class IVa mechanism



Class IVb mechanism



For hydrogen peroxide reacting by a Class IVa mechanism, substrate oxidation occurs as a result of the strongly oxidizing hydroxyl radicals being produced. Fenton⁹ chemistry falls into this category. One disadvantage of catalytic oxidation through this mechanism is that much of the hydrogen peroxide is lost through decomposition. Yields based on peroxide (or peroxide efficiency) are generally less than 10% for Fenton chemistry. For alkyl hydroperoxides and metal alkylhydroperoxides (such as those generated by the Class I mechanism) decomposition produces alcohol and ketones as products, via the Haber-Weiss mechanism.¹⁰ This mechanism is explained more fully in references 1 and 2.

In the Class IVb mechanism, the active oxidant formed is a metal-bound peroxy, hydroperoxy, or alkylperoxy. This bound peroxide reacts with the substrate to produce the oxidized products. This mechanism does not involve peroxide decomposition, and therefore has the potential of giving much higher peroxide efficiency than the Class IVa mechanism.

Class V mechanism

In a Class V mechanism the oxidizing species is the transition metal center. The function of the dioxygen in this type of oxidation mechanism is to regenerate the high oxidation state of the metal complex, either directly or through a co-catalyst. One example of this type of catalysis is the Wacker Process,¹¹ which uses a palladium catalyst to oxidize ethylene to acetaldehyde using dioxygen.

Peroxide Activation

As mentioned earlier, the direct reaction of hydrogen peroxide with most organic substrates is very slow. However, there are several strategies to increase its reactivity. When we talk about “peroxide activation” we are referring to increasing the rate of oxidation in a reaction involving hydrogen peroxide. This activation can involve one of three general routes.¹²

The first route, direct activation, involves the formation of hydroperoxyl and hydroxyl radicals from the hydrogen peroxide. This can be accomplished in several different ways. One way is through the use of UV light to cleave the hydrogen peroxide into two hydroxyl radicals. Another way is through a Class IVa mechanism, (where RO_2H is hydrogen peroxide) which forms the strongly oxidizing hydroxyl radicals through decomposition of the hydrogen peroxide by a transition metal complex.

The second route, activation via peracids, involves the formation of a peracid species from the reaction of hydrogen peroxide with an organic acid. This is an equilibrium reaction, as shown below



The peracid formed is more kinetically reactive than the peroxide alone and is able to oxidize a much wider variety of substrates. Epoxidized soya bean oil, a plasticizer and stabilizer for polyvinyl chloride, is produced by in situ generation of peracetic acid from acetic acid and hydrogen peroxide. Activation via peracids is also utilized in at least one commercial detergent formulation, Tide[®] with Bleach.

The third route, catalytic activation with transition metal complexes, involves the reaction of the transition metal complex with hydrogen peroxide to form the active oxidant. This type of activity is distinct from direct activation because the metal complex, or an oxo or peroxo species bound to the metal complex, is the active oxidant rather than the decomposition products of hydrogen peroxide. Class III, IVb, and V mechanisms for catalytic oxidation can involve the activation of hydrogen peroxide by this route.

Transition metal complexes which activate hydrogen peroxide through the third route, catalytic activation with a transition metal complex, are the focus of the research presented in this dissertation.

•

CHAPTER 2 PEROXIDE ACTIVATION WITH A STERICALLY HINDERED RUTHENIUM COMPLEX

Introduction

There are many applications for metal catalysts that are capable of activating H_2O_2 for oxidations in aqueous solution.¹² Paper pulp bleaching, fine chemical production, and cleaning products are a few of the more obvious examples. Progress has been made in the activation of hydrogen peroxide under laundry conditions, leading to a hypochlorite free detergent formulation.^{13,14} Our emphasis in this chapter is on the pH dependence of peroxide activation by catalysts that function by undergoing redox changes. This corresponds to reactions that are catalyzed by Class III, Class IVa, or Class V mechanisms,^{1,2} discussed in the introduction. The Class III mechanism involves the reaction of a transition metal complex with hydrogen peroxide to form a high-valent metal-oxo complex. Class IVa reactions utilize a transition metal complex to catalytically decompose hydrogen peroxide, generating hydroperoxyl and hydroxyl radicals. These radical species are responsible for the oxidations that occur in a Class IVa mechanism. In a Class V mechanism, the metal center itself is the oxidant. This is distinct from Class III, as in the Class III mechanism the oxidation involves an oxygen atom transfer from the metal-oxo to the substrate. The design of a catalyst system which activates hydrogen peroxide in aqueous solution is complicated by the fact that the peroxide reduction potentials, the redox potential of many metal complexes, and the redox chemistry of substrate oxidation

can all be pH dependent.

Ruthenium complexes, in particular, have received substantial attention as oxidation catalysts. These complexes are reported to exist in a wide range of oxidation states and can form stable oxo and di-oxo species in solution through proton-coupled electron transfer reactions. Che,¹⁵ Meyer,¹⁶ Takeuchi,¹⁷ and Groves¹⁸ and their coworkers have extensively examined the synthesis, reactivity, and electrochemical properties of a large number of these ruthenium complexes.

Research in our laboratories on this area has concentrated on using ruthenium complexes as oxidation catalysts for activation of dioxygen and hydrogen peroxide.¹⁹ For this purpose a sterically hindered ruthenium complex, $[\text{Ru}(\text{DMP})_2(\text{H}_2\text{O})_2]^{2+}$, is employed. This complex is oxidized by hydrogen peroxide and/or dioxygen to form high valent oxo-ruthenium(IV) and the *cis*-dioxo ruthenium(VI). The sterically hindering ligand prevents the formation of μ -oxo dimers and the *trans*-dioxo species, which in other polypyridyl complexes was determined through electrochemical investigations to be a weaker oxidant than the *cis*- complex.^{15d,16a,d,g,20}

An earlier paper^{19a} reported a mechanism for the catalytic oxidation of alkenes and alkanes with dioxygen and hydrogen peroxide. This chapter focuses on the kinetics of formation and thermodynamic oxidizing potentials of the various aquo- and oxo- Ru-DMP complexes. The pH dependence of the ruthenium potentials in aqueous solution is reported and compared to the pH dependent potentials required for the activation of dioxygen and for hydrogen peroxide. In this comparison, thermodynamic implications for the Ru-DMP complexes involved in aqueous catalytic oxidation mechanisms are

discussed. A rate constant for the reaction of the ruthenium(II) with hydrogen peroxide is also reported, and the effect of pH on this reaction examined and compared to the electrochemical results. The discussion presented here is intended for comparison with mechanisms for other reported systems which propose oxidized metal complexes to activate peroxide and/or dioxygen in aqueous solution.

Of the active species formed when hydrogen peroxide reacts with our ruthenium(II) complex, the cis-dioxo ruthenium(VI) species is the most potent oxidant. It is able to oxidize a variety of substrates, including methane.¹⁹ The oxidation of alkanes involves a hydrogen atom abstraction as the first step. The second step is either a radical rebound to generate coordinated ROH or reaction of the radical with O₂ to generate RO₂. For the rebound mechanism, the ruthenium dioxo complex is converted to the [Ru^{IV}(DMP)₂(H₂O)(O)]²⁺ mono-oxo complex. The reduced complex is then reoxidized to the dioxo by hydrogen peroxide.

A general scheme will be presented in this chapter to illustrate the redox considerations essential in transition metal catalyst selection for hydrogen peroxide and O₂ activation in aqueous solution. These considerations apply to catalysts that function by a redox mechanism. The competition that exists between metal redox reactions with H₂O₂ to give the oxidized form of the metal complex for substrate oxidation and reactions of the complex that lead to peroxide decomposition are discussed. The redox analyses and generalizations presented are relevant to understanding metal catalyzed aqueous phase oxidations in commercial and biological systems. Extension of these considerations to

non-aqueous systems requires determination of the corresponding potentials in the solvent system employed.

Experimental

Materials

RuCl_3 , 2,9-dimethyl-1,10-phenanthroline (DMP), LiClO_4 , and LiCl were all used as received from Aldrich. The potassium hydrogen phthalate (Fisher) was dried overnight at 100°C under vacuum. The H_2O_2 (Fisher, 30%) was diluted to the appropriate concentration for the kinetic studies, and the concentration of peroxide checked by iodometric titration. The KOH solution used in the titrations was prepared by dilution of a stock solution made from KOH pellets, followed by standardization with potassium hydrogen phthalate.

Measurements

UV-Vis measurements were performed on a lambda-6 spectrophotometer from Perkin-Elmer. pH measurements were made with a Fisher Accumet model 630 pH meter. Cyclic voltammetry was done with a PAR 173 potentiostat/galvanostat attached to a PAR 175 universal programmer, a PAR 179 digital coulometer, and a Houston Instruments omnigraphic 2000 XY-recorder. The reference electrode was a Corning Ag/AgCl general purpose electrode. The working electrode was a Cypress Systems glassy carbon mini-electrode. Cyclic voltammetry measurements were done in aqueous solution with LiClO_4 as the supporting electrolyte in 0.1 M concentration. The concentration of the complex in the aqueous solution was 1.0×10^{-4} M. pH was adjusted to the appropriate level by adding small amounts of dilute KOH to the solution, the amount of KOH solution added is

sufficiently small that the change in solution volume is negligible. Cyclic voltammograms were obtained at many different pH levels, ranging from 2.42 to 9.90, using a scan rate of 200 mV/sec and a glassy carbon working electrode, against an Ag/AgCl standard electrode.

Synthesis

$\text{Ru}(\text{DMP})_2\text{Cl}_2$ was synthesized by previously published methods.²⁰ Analysis: calc. for $\text{Ru}(\text{DMP})_2\text{Cl}_2$: C, 55.45 ; H, 4.29 ; N, 9.24. Found: C, 55.69 ; H, 3.95 ; N, 8.96.

$[\text{Ru}(\text{DMP})_2(\text{H}_2\text{O})_2](\text{PF}_6)_2$ was synthesized by a modification of the literature procedures.^{19a,20} $\text{Ru}(\text{DMP})_2\text{Cl}_2$ (0.5 g) was suspended in 200 mL of distilled water, and then heated to 70 °C. At the higher temperature, water displaces the chloride ligand, resulting in an orange solution of the diaquo complex. To this, 50 mL of saturated NaPF_6 solution in 0.1 M HPF_6 was added. The solution was then cooled in an ice bath to precipitate the product. The resulting orange-red microcrystals were then filtered and rinsed with 0.1 M HPF_6 solution, then with water. Rinsing continued until the filtrate obtained was free of chloride (AgNO_3 test).

Determination the Oxidation Rate of $[\text{Ru}(\text{DMP})_2(\text{H}_2\text{O})_2]^{2+}$

The procedure for determining the rate of oxidation of $[\text{Ru}(\text{DMP})_2(\text{H}_2\text{O})_2](\text{PF}_6)_2$ by H_2O_2 was to place 3 mL of solution (aqueous) containing a known concentration of the complex (pH = 3.3 for the rate law study) in a spectrophotometer cell and then add 0.5 mL of aqueous hydrogen peroxide solution. The cell was then capped and shaken thoroughly to insure complete mixing and then placed in the spectrophotometer. The absorbance at 495 nm over time was observed and the concentration of the ruthenium(II)

complex was determined as a function of time. The experiments were carried out at room temperature, and the ionic strength was assumed to be constant. Additional experiments demonstrated that a tenfold increase in ionic strength, by addition of KCl, does not significantly alter the rates. This experiment also showed that the addition of excess chloride to the reaction solution did not adversely affect the complex in the timeframe of the experiment. The pH was measured after the conclusion of the experiment and was found to remain constant.

In order to determine the change in concentration of ruthenium(II), a correction accounting for the absorbance of oxidized ruthenium species was made. Reference 5b shows that as peroxide is added to the ruthenium(II) complex, the ruthenium(III) complex is first formed. As the amount of added peroxide increases, the ruthenium(IV) complex and ruthenium(VI) complex are formed sequentially. Isobestic points are observed for each step, and from analysis of the UV-Vis data molar absorptivity, ϵ , values for the ruthenium(II) and (IV) species can be obtained. These are 6870 for the ruthenium(II) and 3540 for the ruthenium(IV) complex. The concentration of ruthenium(II) and the approximate rate constants for our experiment result from the measured absorbance using Equation (2-1).

$$[\text{Ru}^{\text{II}}] = \frac{Ab - \epsilon_{\text{IV}} [\text{Ru}^{\text{II}}]_i}{\epsilon_{\text{II}} - \epsilon_{\text{IV}}} \quad (2-1)$$

The equation (2-1) above was derived as follows:

Let A_t = absorbance at time t

$[\text{Ru}^{\text{II}}]_t$ = concentration of ruthenium(II) at time t

$[\text{Ru}^{\text{II}}]_i$ = initial concentration of ruthenium(II)

ϵ_n = molar absorptivity of ruthenium(II)

Then,

$$A_t = [\text{Ru}^{\text{II}}]_t (\epsilon_{\text{II}}) + [\text{Ru}^{\text{IV}}]_t (\epsilon_{\text{IV}}) \quad (1a)$$

$$[\text{Ru}^{\text{II}}]_i = [\text{Ru}^{\text{II}}]_t + [\text{Ru}^{\text{IV}}]_t \quad (1b)$$

combining (1a) and (1b) gives

$$A_t = [\text{Ru}^{\text{II}}]_t (\epsilon_{\text{II}} - \epsilon_{\text{IV}}) + [\text{Ru}^{\text{II}}]_i (\epsilon_{\text{IV}}) \quad (1c)$$

Therefore,

$$[\text{Ru}^{\text{II}}]_t = \frac{A_t - [\text{Ru}^{\text{II}}]_i (\epsilon_{\text{IV}})}{\epsilon_{\text{II}} - \epsilon_{\text{IV}}}$$

Experimental Results

Three separate experiments were performed to characterize the redox chemistry of the $[\text{Ru}(\text{DMP})_2(\text{H}_2\text{O})_2]^{2+}$ complex. First, an electrochemical study was performed in aqueous solution to determine the change in reduction potentials as the pH changed. Second, $[\text{Ru}(\text{DMP})_2(\text{H}_2\text{O})_2]^{2+}$ was titrated with aqueous sodium hydroxide to determine the pKa of the coordinated water. The titration measurements are related to the pH dependence of the electrochemical results. Third, the titration and electrochemical results are coupled to the peroxide potentials to predict the reactivity of the complex at different pHs and these predictions are examined experimentally.

Electrochemical Results

Figure 2-1 shows a typical cyclic voltammogram for the complex at pH 9.9. While the separation between the cathodic and anodic peaks is slightly greater than 60 mV, the equality of the cathodic and anodic peak currents suggests quasi-reversibility as $(i_p, a/i_p, c) \sim 1$.^{17b} Other reports of electrochemical results from similar complexes report quasi-reversible or irreversible couples with a glassy carbon electrode.^{15g} The $E_{1/2}$ values for the ruthenium redox couples from cyclic voltametry studies were obtained for a wide pH range and are shown in Table 2-1. The reported values have been adjusted to standard reduction potentials by adding 0.197 V to the values obtained with the Ag/AgCl reference.²¹ These reduction potentials are for a 1.0×10^{-4} M solution of the metal complex.

At pH 5.8 and above, oxidations attributed to the III/II, IV/III and VI/IV couples are observed. At lower pH values, only two redox steps are distinguished. The III/II and VI/IV couples are sensitive to pH and the other couples are relatively insensitive. The columns labeled as the "IV/II" couple in Table 2-1 refers to the $E_{1/2}$ value where the III/II and IV/III couples merge into one peak.

Electrochemical measurements of this complex in aqueous solution below pH 3 have been previously reported²⁰ and, for the most part, agree with those reported here. We were not able to see the clear separation of the III/II and IV/III oxidations

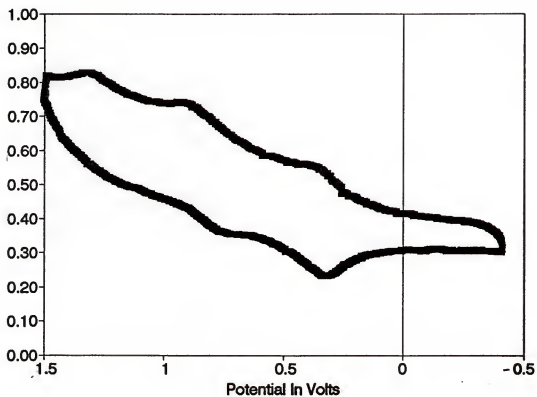


Figure 2-1: A typical cyclic voltammagram, the one shown here is for the $[\text{Ru}(\text{DMP})_2(\text{H}_2\text{O})_2]^{2+}$ complex at pH = 9.90. The scale shown is for potential vs. the Ag/AgCl reference.

Table 2-1: The $E_{1/2}$ values for the ruthenium complex at different pH levels. These values have been adjusted to reflect voltages vs. SHE.

pH	III/II	IV/II	IV/III	VI/IV
9.90	0.747	---	1.05	1.52
8.24	0.747	---	1.05	1.52
7.12	0.772	---	1.05	1.52
6.49	0.847	---	1.05	1.52
5.78	0.872	---	1.05	1.52
5.19	---	1.02	---	1.52
4.60	---	1.02	---	1.52
3.74	---	1.05	---	1.52
3.09	---	1.06	---	1.60
2.42	---	1.06	---	1.70

reported at low pH nor did we observe the V/IV couple. The other reported $E_{1/2}$ values are in good agreement with ours.

Titration Results

The solution pH was monitored for the $[\text{Ru}(\text{DMP})_2(\text{H}_2\text{O})_2](\text{PF}_6)_2$ as it was titrated with standardized $\text{KOH}(\text{aq})$ solution. The resulting titration curve, Figure 2-2, exhibits two clear inflection points. One occurs at the addition of one mole of $\text{KOH}(\text{aq})$ per mole of ruthenium complex. The second inflection occurs after two moles of $\text{KOH}(\text{aq})$ have been added per mole of ruthenium, reflecting the sequential deprotonation of two aquo ligands. The pK_a values measured from these inflections are 3.28 and 5.13. These pK_a values are much lower than those reported by Meyer and coworkers^{16,22} and Che^{15c,d,f,g} for coordinated water to a ruthenium(II) center. The pK_a values we report are closer to those reported by Che and coworkers^{15c,d,f,g} for coordinated water in *trans*-diaquoruthenium(III) complexes. Steric effects cause the DMP ligand to be more loosely bound in our complex, making the ruthenium center more electrophilic and therefore binding the water more strongly. Evidence to support the DMP being more weakly bound is given by the electrochemical results. The reduction potentials for the high valent *cis*-dioxo ruthenium(VI) complexes are known to be higher (by over 200 mv)^{15d,e} than those of the *trans*-species. In addition, the DMP complex of ruthenium shows an unusually high (VI)/(IV) reduction couple compared to the *cis*-bipyridine derivative complexes of ruthenium.^{15e} Our assertion is that the low degree of high-oxidation state stabilization, as evidenced by our electrochemical results, indicates that interaction between the

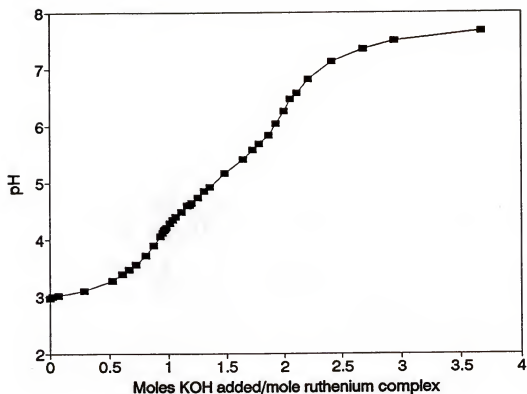


Figure 2-2: The titration curve of the ruthenium complex. Note the inflection points of the curve. Analysis of these inflections gives pKa values for the coordinated water as 3.28 and 5.13.

ruthenium center and the DMP ligand is unusually weak. This results in a more electrophilic ruthenium center which binds the water more strongly and results in much lower pK_a values than those in the literature for ruthenium(II) complexes.

In this system, the first conjugate base produced is $[Ru^{II}(DMP)_2(H_2O)(OH)]^+$ and the species formed after removal of the second proton is proposed to be $Ru^{II}(DMP)_2(OH)_2$. Unfortunately, the UV-Vis spectrum does not change significantly with pH, as mentioned below, and the pK_a values could not be correlated to direct spectral changes.

Oxidation of the Ruthenium Complex by Hydrogen Peroxide

The spectral changes that occur in the reaction between the $[Ru(DMP)_2(H_2O)_2]^{2+}$ complex and hydrogen peroxide lead to a decrease in the strong absorbance at 495 nm for the ruthenium(II) complex in aqueous solution.^{5b} Figure 2-3 shows a typical absorbance versus time curve for the reaction of hydrogen peroxide and our ruthenium complex. The initial rates of the reaction between hydrogen peroxide and the ruthenium complex, measured for a series of different ruthenium and peroxide concentrations, are given in Table 2-2. The initial rate was determined by calculating the difference in concentration of the ruthenium(II) species over the first 10 seconds of the reaction. From these initial rates, an empirical rate law can be determined.²³ The resulting rate law for the decrease in ruthenium(II) is first order in peroxide and ruthenium concentrations. This empirical rate law is expressed in Equation (2-2).

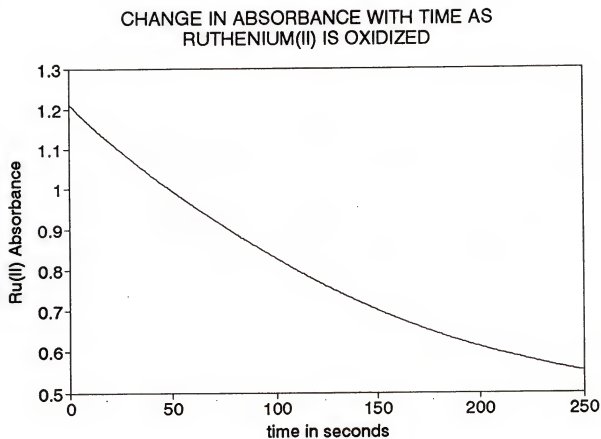


Figure 2-3: A typical UV-Vis kinetic run for the oxidation of the ruthenium complex by hydrogen peroxide. The ruthenium complex absorbance at 495nm is measured as a function of time after the addition of hydrogen peroxide to the cell.

$$-d[\text{Ru}^{\text{II}}]/dt = 0.3 [\text{Ru}^{\text{II}}] [\text{H}_2\text{O}_2] \quad (2-2)$$

The reaction of $[\text{Ru}(\text{DMP})_2(\text{H}_2\text{O})_2]^{2+}$ with hydrogen peroxide was observed for a range of pH values. The initial rate of oxidation does not vary significantly as the pH changes. However, as can be seen in Figure 2-4, as the pH is increased from 3.33 to 9.13, the reaction extent decreases. At lower pH levels, i.e. pH = 4 and below, the Ru^{II} is almost completely oxidized to Ru^{VI} . However, as the pH increases, the reaction seems to proceed to only the Ru^{IV} species. As the molar absorptivity of the Ru^{IV} is between that of the Ru^{II} and Ru^{VI} species, we would expect a smaller decrease in absorbance when Ru^{IV} is the product. Reasons behind this behavior are explained in the discussion section.

Discussion

Metal Complex Activation of H_2O_2

The reactivity of H_2O_2 with $[\text{Ru}(\text{DMP})_2(\text{H}_2\text{O})_2]^{2+}$ and the ability of the resulting system to catalyze substrate oxidation in aqueous solution is governed by the pH dependence of the metal complex and hydrogen peroxide reduction potentials. In this section, generalizations will be presented concerning the reactivity of hydrogen peroxide with metal complexes. These concepts will then be used to interpret the results of the reaction of $[\text{Ru}(\text{DMP})_2(\text{H}_2\text{O})_2]^{2+}$ with H_2O_2 and the pH dependence of this system for substrate oxidation. The conditions for efficient activation of hydrogen peroxide by a transition metal complex in aqueous solution will be discussed first.

Table 2-2: Initial rates for the oxidation of the ruthenium complex by hydrogen peroxide.

Run #	$[\text{H}_2\text{O}_2]^a$	$[\text{Ru}(\text{DMP})_2(\text{H}_2\text{O})_2^{2+}]^a$	Initial Rate ^b
1	0.0660	1.15×10^{-4}	1.90×10^{-6}
2	0.0264	1.15×10^{-4}	9.85×10^{-7}
3	0.0106	1.15×10^{-4}	4.15×10^{-7}
4	0.00577	1.15×10^{-4}	2.24×10^{-7}
5	0.00211	1.15×10^{-4}	1.05×10^{-7}
6	0.0264	6.90×10^{-5}	6.55×10^{-7}
7	0.0264	4.60×10^{-5}	3.50×10^{-7}
8	0.0264	3.30×10^{-5}	2.15×10^{-7}

^aAll concentrations are in units of moles per liter.

^bThe initial rates are in units of moles $[\text{Ru}^{2+}] \text{ L}^{-1} \text{ S}^{-1}$. These initial rates were determined by a linear regression performed on the data from the first 10 seconds of the kinetic runs. In all cases, the R^2 value was 0.99 or better, insuring linearity.

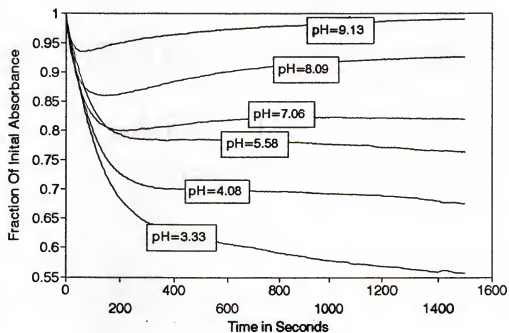
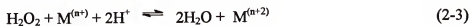


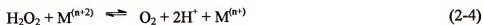
Figure 2-4: A comparison of the kinetic curves for the ruthenium oxidation with changes in pH. Note the similarity of initial rates, and the inability of the peroxide to completely oxidize the complex at higher pH values.

The general scheme for understanding the reactions which occur when a transition metal complex and hydrogen peroxide interact is obtained by examining the half-reactions for the oxidation and reduction of hydrogen peroxide. The reaction for the reduction of hydrogen peroxide by a metal ion to form water (and thus oxidizing the metal complex) is given in Equation (2-3).



This reaction, peroxide reduction and metal oxidation, is involved in substrate oxidation by Class III or V mechanisms or in alkyl peroxide decomposition by a class IVa mechanism. In the Class III reaction, the metal undergoes the two electron transfer, shown in Equation (2-3). Catalysis by the metal complex occurs when the oxidized metal complex, metal peroxo, or metal oxo species is kinetically more reactive than peroxide in the oxidation of substrate.

The oxidized complex may undergo the reaction with hydrogen peroxide shown in Equation (2-4). This reaction involves the oxidation of hydrogen peroxide and the reduction of the metal complex.



Thus, depending on the potentials of the oxidized and reduced forms of a given metal complex catalyst, both peroxide reduction and peroxide oxidation can occur, leading to

the catalyzed decomposition of hydrogen peroxide to water and dioxygen. This nonproductive oxidation of hydrogen peroxide competes with substrate oxidation for the oxidized metal complex and leads to a waste of the H_2O_2 .

A quantitative evaluation of the free energies ΔG ($\Delta G = nFE$) involved in metal catalyzed activation of H_2O_2 for substrate oxidation requires knowledge of the reaction potentials at the conditions of the experiment. These potentials or required equilibrium data are seldom available for nonaqueous solvents. The approach presented here involves the correlation of observed reactivity in aqueous solution with the standard reduction potentials. If the results correlate, electrochemical considerations can be used to modify the catalyst system to improve its activity and efficiency. It is also important to remember that a small positive free energy or negative potential for an oxidation reaction corresponds to small equilibrium concentrations of an oxidized catalyst. Small concentrations of very active catalysts can lead to significant oxidation rates.

The reduction potentials²⁴ in acid ($\text{pH}=0$) solution for the half reactions involving hydrogen peroxide are given in Equations (2-5) and (2-6).



The pH dependence of these potentials using aqueous solution, calculated with the

Nernst equation,²⁵ is shown in Figure 2-5.* The potential for peroxide being reduced (i.e. the peroxide half-reaction when it oxidizes the transition metal complex), is given by line A. The reduction potential for the reaction that involves peroxide oxidation (i.e. its reaction in nonproductive, metal complex reduction) is given by line B in Figure 2-5. This line also corresponds to the reduction potential for the two electron reduction of O₂ to H₂O₂.

For the reactions in the catalytic cycle to proceed spontaneously with H₂O₂, the E° for Equation (2-3) must be positive. Since the metal half-reaction is oxidation, the metal reduction potential must be a smaller positive number than the peroxide reduction potential given by line A in order to have a negative free energy (i.e. positive E) for Equation 2-3. If a metal complex has a reduction potential that is more positive than the peroxide reduction potential at a given pH, that complex cannot be oxidized by H₂O₂, because the free energy for the reaction will be positive. For this reason, many strong oxidizing agents that undergo stoichiometric oxidations of organic substrates are not catalysts because they cannot be reoxidized by peroxide.

* The reduction potentials for these reactions can be found at any pH by employing the Nernst equation, shown below, to adjust for H⁺ concentration below 1.0 M.

$$E = E^{\circ} - \frac{2.303 R T \log Q}{n F}$$

where Q, the reaction quotient, is expressed by

$$Q = \frac{[H_2O]^2}{[H_2O_2][H^+]^2}$$

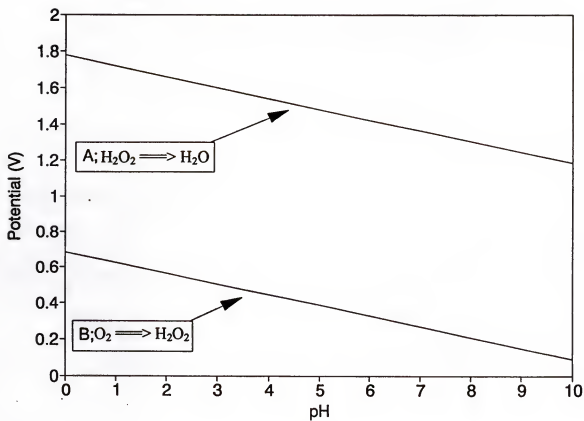


Figure 2-5: The pH dependence of the half-reaction potentials for the reduction (A) and the oxidation (B) of hydrogen peroxide.

To generate the strongest catalytic oxidant for the activation of hydrogen peroxide, the reduction potential for the metal complex should be as high as possible without exceeding the reduction potential of hydrogen peroxide at that pH (curve A). Comparable potentials make reaction (2-3) spontaneous and produce a metal complex that is almost as good an oxidizing agent in a thermodynamic sense as H_2O_2 .

Line B of Figure 2-5 illustrates the pH dependence for the reduction potential for the half-reaction in which H_2O_2 is oxidized to O_2 . When the potential for Equation (2-4) is positive, peroxide will be oxidized and the transition metal complex reduced. Equation (2-4) is spontaneous when the metal reduction potential has a larger positive value than line B of Figure 2-5. If both reactions (2-3) and (2-4) are spontaneous with the same metal complex, then that complex will catalytically decompose hydrogen peroxide as explained above. Figure 2-5 shows that any metal that can be oxidized to produce a metal oxidant that is as good an oxidant as H_2O_2 (i.e. has a reduction potential close to that for H_2O_2 reduction to water) will lead, on thermodynamic grounds, to nonproductive decomposition of H_2O_2 . The graph summarizes the pH dependence of the peroxide couples and can be readily utilized with the metal reduction potentials to produce the free energy sign of Equations (2-3) and (2-4).

In order to avoid the reaction in Equation (2-4), the metal reduction potential of the oxidized form of the complex, and hence the "oxidizing power" of the oxidized metal complex, must be below the potential shown in line B of Figure 2-5. This produces an oxidized form of the catalyst that is a much poorer oxidizing agent (in a thermodynamic sense) than H_2O_2 . However, the resulting oxidant is still as strong as that resulting from

the two electron reduction of O_2 . If the resulting oxidant is able kinetically to oxidize the desired substrate by Class II, III or V mechanisms, efficient utilization of peroxide or O_2 can result. Based on thermodynamic considerations, any metal complex that utilizes hydrogen peroxide to produce a high oxidation state metal complex **cannot** be both as strong an oxidant as hydrogen peroxide and also efficiently use hydrogen peroxide. Kinetic paths must be found to obtain an efficient catalyst. Unfortunately, these higher potentials are necessary to generate electrophilic metal oxo species needed for a Class III mechanism.

Very strong oxidizing catalysts for peroxide activation could result if favorable kinetic barriers reduce the rate of the peroxide oxidation reaction (Equation (2-4)). Low concentrations of peroxide compared to substrate lead to conditions where oxidation of peroxide competes less favorably with oxidation of substrate in the reaction with the oxidized form of the catalyst. Non-labile ligands in the oxidized complex can inhibit peroxide coordination and inner sphere electron transfer paths. Outer sphere electron transfer mechanisms are more likely to lead to slower metal reduction by peroxide.

Figure 2-5 has implications for understanding the behavior of metal oxidases. At standard conditions O_2 is not able to oxidize any metal complex whose reduction potential is much above line B in Figure 2-5. If a sacrificial two electron reducing agent can be used to convert O_2 to H_2O_2 , any metal complex with a reduction potential below line A in Figure 2-5 can be oxidized and can function as a catalyst for substrate oxidation. The kinetically favored systems are labile complexes where H_2O_2 can displace a coordinated water in the low oxidation state. These thermodynamic considerations explain the role of

the sacrificial reducing agent in mono-oxygenase type systems. Without the sacrificial reducing agent to form peroxide, O_2 is not able to oxidize metal complexes whose reduction potential are between lines A and B in figure 2-5.

The pH Dependence of Peroxide Activation by $[Ru(DMP)_2(H_2O)_2]^{2+}$

The discussion presented above provides the framework for selecting metal complexes to activate hydrogen peroxide at different pH values for substrate oxidation in aqueous solution. In this section they will be applied to the $[Ru(DMP)_2(H_2O)_2]^{2+}$ complex. First, consider the free energy of oxidation of the complex $[Ru(DMP)_2(H_2O)_2]^{2+}$ by H_2O_2 , Equation (2-3). For this purpose, the pH dependent potential for oxidizing ruthenium must be considered as well as the pH dependent potentials for reducing peroxide. The pH titration has shown that at different pH values $[Ru(DMP)_2(H_2O)_2]^{2+}$, $[Ru(DMP)_2(H_2O)(OH)]^+$ and $Ru(DMP)_2(OH)_2$ exist in solution. This chemistry gives rise to a pH dependence of the metal complex redox potential. In Figure 2-6, the ruthenium reduction potentials are indicated by solid lines that are superimposed on the peroxide potentials (dashed lines) from Figure 2-5.

As can be seen, the oxidation of ruthenium(II) to ruthenium (IV) by H_2O_2 is spontaneous at all pH values shown. The reduction potential for the ruthenium (IV)/(II) and (III)/(II) couples both are lower than the reduction potential of hydrogen peroxide. However, as we get to higher pH levels, the reduction potential of H_2O_2 is too low (i.e. H_2O_2 is not a good enough oxidizing agent) to oxidize ruthenium (IV) to ruthenium (VI). As the pH rises above 5, the ruthenium (VI) complex is formed in diminishing amounts. This chemistry accounts for the pH dependence of the oxidation of $[Ru(DMP)_2(H_2O)_2]^{2+}$

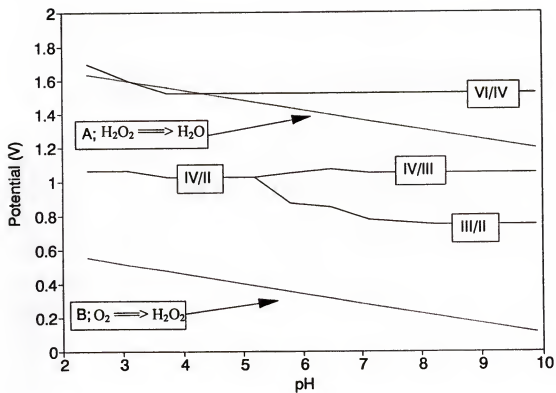


Figure 2-6: A comparison of the ruthenium reduction potentials (solid lines) and the potentials for oxidation and reduction of hydrogen peroxide (dashed lines).

by peroxide shown in Figure 2-4. As the pH increases, the amount of Ru^{VI} formed decreases, and a smaller decrease in absorbance is observed.

Next, let us consider the ability of the high oxidation state ruthenium complexes to oxidize and thus decompose H_2O_2 . For this purpose, the metal reduction potentials (indicated by the solid line) are compared to the dotted line indicating the reduction potential of the reaction involving peroxide oxidation. As stated earlier, metal reduction potentials for the oxidized metal complex that will result in the spontaneous oxidation of H_2O_2 are those which are more positive than those reduction potentials on line B. Under all pH conditions, the reduction potential of the ruthenium (IV) and ruthenium (VI) complexes have the thermodynamic potential to oxidize hydrogen peroxide. The efficient use of peroxide in the catalytic reactions of this complex is attributed to a slow kinetic pathway for peroxide oxidation / metal reduction. The nucleophilic oxygen of peroxide is more likely to displace water from the (II) oxidation state than to displace aquo or hydroxo ligands from the (IV) oxidation state complex. The reason for this is that, while the (IV) and (VI) are more electrophilic, the ruthenium (II) is much more labile to substitution than the higher valent complexes. The aquo and/or hydroxide ligands on the ruthenium (IV) are not likely to be removed at all. Rather, it is likely that a proton-coupled electron transfer occurs at this point. Proton-coupled electron transfer has been seen in similar complexes.^{15e,16a,b} Thus, the ruthenium(II) complex is oxidized faster by peroxide than the ruthenium (IV) or (VI) complex is reduced.

Conclusions on the *rates* of competitive reactions cannot be based on thermodynamic considerations alone. For example, from figure 2-6 we can conclude that

at pH 3, the reaction of hydrogen peroxide with ruthenium (IV) is spontaneous for both the formation of ruthenium (II) and (VI). In using the potentials for the ruthenium complex and hydrogen peroxide to find the free energy change of each reaction we find that the oxidation of the peroxide to form the ruthenium (II) complex is favored thermodynamically over the reduction of the peroxide to form the ruthenium (VI) complex. However, from earlier spectrophotometric studies,^{19b} we know that the reaction to form the ruthenium (VI) species is the favored reaction. Thus, kinetic considerations facilitate the reaction to produce ruthenium (VI).

The analysis presented here has significant implications for mechanistic considerations in aqueous solution. If the reduction potential for metal complex oxidation becomes significantly more positive than the peroxide or O_2 reduction potential, substrate oxidations through Class III and V mechanisms are not possible. If substrate oxidation occurs, a Class IV mechanism involving nucleophilic attack on a coordinated peroxide is suggested. When the oxidized form of the metal complex has a reduction potential below that of O_2 , the pH dependence of the metal complex potential and the pH dependence of substrate oxidation should be used to construct a graph similar to Figure 2-6 to ascertain the pH dependence of the catalysis. The metal complex must remain soluble for these considerations to be relevant and this is often a problem at higher pH.

pH Dependence of Methane Oxidation

It is informative to illustrate the application of the above considerations to the oxidation of methane to methanol to illustrate the thermodynamic considerations for this reaction. The reduction potential for methanol is shown below.²⁶



The Nernst equation shows that this reduction potential falls to -0.013 V at pH = 10.

The first consideration involves comparing the substrate potentials with those available for H_2O_2 to determine if the reaction is feasible at different pH values in aqueous solution.

The methane oxidation potential falls below the line marked B (on figure 2-5) at all pH values from zero to ten (0.58 V at pH of 0 and -0.013 V at pH of 10). The implication of this is that at all pH values methane can be oxidized by O_2 and is thermodynamically easier to oxidize than hydrogen peroxide. It would be possible, thermodynamically, to use hydrogen peroxide with 100% efficiency to oxidize methane over the pH range 0 to 10 when the oxidized metal is too weak an oxidant to oxidize hydrogen peroxide, but has a large enough reduction potential to oxidize methane spontaneously.

Figure 2-7 shows the pH dependant reduction potentials for the peroxide/dioxygen half reaction on the same graph as the reduction potentials involved in methane oxidation. As can be seen, the methane reduction potential is lower at all pH levels than the peroxide/dioxygen potential. If a transition metal complex were to have a two-electron reduction potential between lying in the area between these two lines, that complex has the possibility for efficient use of peroxide for catalytic methane oxidation. In the area between the potential lines in figure 2-7, the oxidized form of the metal complex would be potent enough an oxidant to oxidize methane to methanol, but would not catalyze decomposition, as it would not be able to oxidize peroxide to dioxygen. The next problem

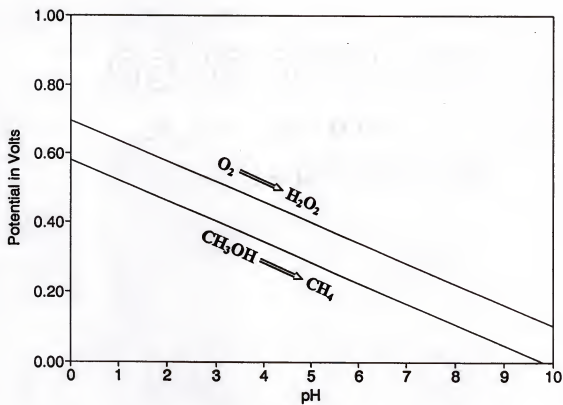


Figure 2-7: A comparison of the reduction potentials for the methane/methanol and peroxide/dioxygen half-reactions.

involves consideration of the redox potential of the metal complex to determine if H_2O_2 can generate the oxidation state required for CH_4 oxidation at all pH values. This is accomplished for the $[\text{Ru}(\text{DMP})_2(\text{H}_2\text{O})_2]^{2+}$ catalyst by adding the $\text{CH}_4/\text{CH}_3\text{OH}$ potential to pH dependence of the complex potentials shown in Figure 2-6. The ruthenium (VI) complex is more than strong enough an oxidant to convert methane to methanol at all pH values. However, ruthenium (VI) is not formed from H_2O_2 above pH 4.5. Interestingly, the ruthenium (IV) complex is thermodynamically strong enough an oxidant to convert methane to methanol. However, for kinetic reasons the (VI) complex is required and the reaction will not occur with H_2O_2 above pH 4-5. If the (IV) oxidation state were active kinetically, the catalysis of the oxidation of methane by hydrogen peroxide would occur over the entire pH range. In order to obtain a kinetically active metal oxo species for hydrogen atom abstraction or oxygen atom insertion into CH_4 , the ruthenium (VI) dioxo complex is needed. This is because the ruthenium (IV) is not sufficiently electrophilic to interact significantly with the C-H sigma bond of methane. The ruthenium (VI) species is able to overcome the kinetic barrier for methane oxidation because it will interact significantly with the C-H bond due to it being much more electrophilic.

Oxidation of Alkenes by $[\text{Ru}(\text{DMP})_2(\text{Soln})_2]^{2+}$ and O_2 .

The epoxidation of alkenes is carried out by O_2 in acetonitrile solution.¹⁹ In the absence of peroxides, the reaction is observed to have a 24 hour induction period. This induction period is eliminated when three equivalents of an alkyl hydroperoxide or hydrogen peroxide are added. Previously we had concluded that alkylhydroperoxide is formed in the induction period, and this reacts to form ruthenium (IV). It was proposed

that ruthenium (IV) is oxidized to the ruthenium (VI) by dioxygen and ruthenium (VI) is the oxygen atom transfer agent. The addition of peroxides eliminated the induction period by oxidizing the ruthenium (II) to the ruthenium (IV).

The redox considerations presented here would indicate that this mechanism may not be correct. Collin and Sauvage report that the IV/II reduction potential for $\text{Ru}(\text{DMP})_2(\text{Solv})_2^{2+}$ (Solv = solvent) changes from 1.0 V in water to 1.7 V in CH_3CN .²⁰

Unfortunately the O_2 reduction potential in most non-aqueous solvents is not known.

However, in view of the high reduction potential in aqueous solution, the postulation of generating a high valent ruthenium(VI) species by O_2 in non-aqueous solutions is suspect.

The following scheme is proposed as an alternative to the generation of a ruthenium(VI) species. Ruthenium (II) is oxidized to ruthenium (III) by hydrogen peroxide, or by alkylhydroperoxide formed in the induction period from alkene autoxidation. The formation, and subsequent decomposition, of the alkylhydroperoxide is indicated by the small amounts of ketone and alcohol formed during the induction period from the alkene when the reaction is carried out with O_2 . These products are not formed after the inductive period. The induction period for the epoxidation reaction in the absence of peroxide is due to the slow rate of autoxidation. Once the ruthenium (III) species is formed, it can be oxidized to the ruthenium (IV) oxo species by dioxygen. Nucleophilic attack by an alkene Ru(IV)O results in oxygen atom transfer to form epoxide and reduction of the metal to form ruthenium (II). The ruthenium (II) complex can react with a ruthenium (IV) to produce two ruthenium (III) complexes. These then react with dioxygen to produce ruthenium (IV) oxo making the reaction catalytic after significant

amounts of ruthenium (IV) exist. The reaction pathways discussed here are shown in figure 2-8 (p.40).

Conclusion

The complex $[\text{Ru}(\text{DMP})_2(\text{H}_2\text{O})_2]^{2+}$ undergoes reaction with hydrogen peroxide that is first order in both ruthenium and peroxide. At pH levels above 3.5-4, the acidic protons of the aquo ligands are neutralized (pK_a of 3.28 and 5.13). The electrochemical experiments confirm this transformation by showing breaks in the $E_{1/2}$ vs. pH graph at the deprotonation pH values. The ruthenium complex is shown not to form significant amounts of the active cis-dioxo complex at pH levels above 5.

Figure 2-5 is proposed as a template upon which substrate and metal ion potentials can be superimposed to predict and explain the reactivity of hydrogen peroxide with any transition metal complex in aqueous solution. The inability of $[\text{Ru}(\text{DMP})_2(\text{H}_2\text{O})_2]^{2+}$ to form $[\text{Ru}(\text{DMP})_2(\text{O})_2]^{2+}$ from hydrogen peroxide at higher pH levels is predicted. Substrates with a kinetic preference for the dioxo complex will show a large pH dependence for their oxidation. The procedures discussed can be used to screen transition metal complexes as peroxide activation catalysts. When free energy signs are estimated and applied to other than standard conditions, qualitative estimates of the influence of these conditions on the relevant potentials should be considered.

CHAPTER 3

ACTIVATION OF HYDROGEN PEROXIDE FOR OXIDATION WITH COPPER(II) COMPLEXES

Introduction

The activation of hydrogen peroxide for the oxidation of organic substrates by transition metal complexes has been studied extensively, and there are many established examples in nonaqueous solvents.²⁷⁻²⁹ Environmental concerns have motivated replacement of aqueous hypochlorite as an oxidant by peroxide, and replacement of nonaqueous solvents as reaction media by water. Few transition metal complexes are effective oxidation catalysts for hydrogen peroxide in aqueous solution, and even fewer are active at pH 8 or above. There are several patents which address this problem.³⁰ At higher pH, the precipitation of the catalytically active metal complex as the oxide or hydroxide is a major limitation. One way to overcome this is through the use of chelating ligands, which stabilize the metal ion in basic solution and prevent precipitation. Recent reports show that a manganese complex of 1,4,7-triazacyclononane (TACN)¹³ is an effective peroxide activator in basic aqueous solution. This complex is demonstrated to catalyze the epoxidation of styrene and 4-vinylbenzoic acid with hydrogen peroxide, and has been commercialized as a bleaching agent for household applications. The development of this system has intensified investigations in the area of transition metal catalyzed peroxide activation. The primary goal of research in this area is to find transition

metal complexes which will react with hydrogen peroxide to produce an active oxidizing agent in basic aqueous solution.

The activation of hydrogen peroxide by redox mechanisms (Classes III, IVa, and V)^{1,2} almost invariably leads to the catalysis of peroxide decomposition. This can be avoided by employing catalysts which function by mechanisms where transition metal center does not change its oxidation state when activating the hydrogen peroxide, such as in a Class IVb mechanism. These reactions involve the coordination of HO_2^- to a metal center and can be viewed as replacing the proton of H_2O_2 with a Lewis acid (the metal complex), and in the process activating HO_2^- . Accordingly, a series of experiments were carried out to find copper(II) complexes that might function as peroxide activators through hydroperoxide coordination.

Copper complexes of bis(ethylenediamine)³¹ and bis(bipyridine)³² have been shown to be active for peroxide activation, although not at basic aqueous conditions. Many copper complexes containing a bound peroxo species are known, however most are dimeric species.³³⁻³⁶ Interestingly, complexes with cumylhydroperoxide and *tert*-butylhydroperoxide species bound to a copper(II) monomer have been isolated³⁷ and found to have O-O bond distances similar to those for other alkylperoxo species used for oxidations.

In this chapter, the activation of hydrogen peroxide by a series of copper(II) complexes is examined. The initial experiments were done using picolinic acid as a ligand, which has been effective in promoting peroxide activation with iron in a pyridine-acetic acid solvent mixture.²⁸ The iron-picolinic acid system was itself based on the earlier Gif

and GoAgg systems.²⁹ After finding significant activity with the copper(II)-picolinic acid complex, we expanded our examination to additional classes of ligands. The substrate oxidation was performed at a pH of 9.1 in a borax buffer unless otherwise indicated. Rate studies, reported as initial rates, were performed and the oxidation rates were measured as a function of pH, peroxide concentration, ligand to metal ratio, and complex concentration. From these results, a mechanism for peroxide activation with complexes of this type is proposed.

Experimental

Materials

Copper(II) chloride and sodium tetraborate were used as received from Fisher. 30% Hydrogen peroxide was used after iodometric titration to verify its concentration. Quinaldine blue, Picolinic acid (PA), acetylacetone (AcAc), glycine (GLY), alanine (ALA), leucine (LEU), dipicolinic acid (DPA), iminodiacetic acid (IDA), ethylenediamine (EN), tetramethylethylenediamine (TMED), 2,9-dimethyl-1,10-phenanthroline (DMP), bipyridylamine (BPA), tris(2-aminoethyl)amine (TREN), iminobis(propylamine) (IBPA), and terpyridine (TERPY) were all used as received from Aldrich. The water used for the peroxide solutions was purified using a barnstead NANOpure unit. The final resistance of the purified water was $18 \text{ megaohm}\cdot\text{cm}^{-1}$. This high level of purity prevents the presence of any metal-ion contaminants that might influence peroxide concentration through decomposition.

Measurements

UV-Vis measurements were performed on a Perkin-Elmer Lambda-6 spectrophotometer. The rate data was obtained through observation of the decrease in quinaldine blue concentration by monitoring the absorbance at 600 nm over time. pH measurements were made with a Fisher Accumet model 630 pH meter.

Preparation Of Reaction Mixtures For Kinetic Measurements

Preparation of the substrate. Quinaldine blue, 0.0060g, was dissolved in a 0.01 M aqueous sodium tetraborate buffer solution. This gives a deep purple solution with an absorbance of between 1.0 and 1.1 at 600nm. The initial absorbance was checked before the solution was used, to insure that the absorbance is in the above range.

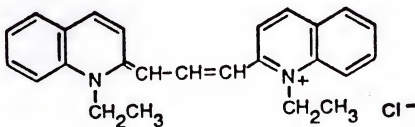
Preparation of the catalysts. The catalyst solution used was prepared from 2.5×10^{-3} M stock solutions of copper(II) chloride and 2.5×10^{-3} M stock solutions of the appropriate ligand. This method of catalyst preparation is similar to the in-situ generation of the active complex in references 28 and 32. Use of the copper(II) nitrate, rather than the copper(II) chloride, as the copper(II) source does not significantly affect the rates, nor did addition of excess chloride to the system. At these concentrations, precipitation was not observed, and the catalyst solutions did not lose activity upon standing.

Preparation of the peroxide solution. A 0.200 M stock solution of hydrogen peroxide was made by adding 10 mL of 30% hydrogen peroxide (whose concentration was checked by iodometric titration) to a 500 mL volumetric flask and diluting with purified (as explained above) water to 500mL. Subsequent dilutions were made to give the

peroxide solutions used. All the rate data presented were obtained using peroxide solutions no more than 48 hours old.

Procedure For The Kinetic Measurements

The oxidation of quinaldine blue [I] was used as the probe reaction to monitor peroxide activation.



I

This material is highly colored, with a UV-Vis absorbance maximum at 600nm that is insensitive to pH changes above pH 4. Quinaldine blue is not oxidized by H_2O_2 at the concentrations used in this research. However, stronger oxidants such as oxone or hypochlorite produce a colorless product which has negligible absorbance at 600nm. Reactions of this substrate are readily monitored with UV/Vis spectroscopy.

In each experiment, 2 mL of the buffered substrate solution, 1 mL of catalyst solution (for blank runs the "catalyst solution" used was water), and 0.5 mL of peroxide solution were added, in that order, to a UV-Vis cell. This combination of buffered substrate solution, copper complex, and hydrogen peroxide has a pH of 9.1. The cell was capped and shaken for 5 seconds and then placed in the cell holder in the UV-Vis, at

which point data collection was initiated. The absorbance at 600nm was monitored as a function of time. As the substrate is oxidized the absorbance at 600nm decreases. The rate of this decrease was measured and the rate of reaction determined using data collected during the first 10 to 20 seconds of reaction. These initial rates of reaction as a function of initial concentrations are given in the results section.

Quinaldine blue has an EPR signal at $g=2.0$, which attests to its radical nature. The colorless, oxidized product exhibits no EPR spectrum and gives an NMR spectrum. There are several products from the oxidation of this substrate.³⁸ The initial step of the oxidation is suggested to involve cleavage of the linkage between the substituted quinoline groups. It is also possible to perform a one-electron oxidation of the quinaldine blue, similar to reactions of 2,2'-azinobis(3-ethylbenzothiazoline-6-sulfonate) (ABTS²⁻).

Quinaldine blue is proposed for general use to study oxidations in aqueous solutions instead of the commonly used ABTS²⁻.³⁹⁻⁴² The ABTS²⁻ is converted to the ABTS^{•-} radical upon one-electron oxidation. This radical species has an intense green color, therefore studies using the ABTS²⁻ as the substrate monitor the progress of the reaction by spectrophotometry. However, in our catalyst systems, further reactions of the ABTS^{•-} radical limited its usefulness. The ABTS^{•-} radical was rapidly oxidized to ABTS, as evidenced by the total disappearance of the green color (characteristic of the ABTS^{•-} radical) from the reaction solution after around 10-30 seconds.

The reactivity of the copper(II) complexes with the quinaldine blue in the absence of peroxide was tested. There have been some reports of copper(II) complexes oxidizing amine containing buffers in aqueous solution without peroxide.^{43,44} The absorbance of

solution containing equimolar concentrations of copper(II) and quinaldine blue showed no change in absorbance with time over a 2-hour period. We therefore conclude that the oxidation of quinaldine blue by the copper(II) center (a class V mechanism) does not occur in the timescale of our experiments.

Results And Discussion

Activation of Peroxide by Copper(II) Chloride and Picolinic Acid

The first set of copper(II) complexes examined as catalysts used picolinic acid as the ligand. The iron complex of this ligand is an effective catalyst for peroxide activation in an acetic acid / pyridine solvent mixture.²⁸ A catalyst solution containing 1.0×10^{-4} moles/liter of picolinic acid and copper(II) chloride, in a 1:1 mole ratio, was found to strongly activate the peroxide for the oxidation of quinaldine blue. The absorbance at 600nm versus time for this reaction is shown in Figure 3-1. Picolinic acid by itself does not catalyze the oxidation of quinaldine blue with hydrogen peroxide. Copper(II) ion, in the absence of a strong-binding ligand, forms the hydroxide under our experimental conditions. Hydrogen peroxide is decomposed on the surface of the copper(II) hydroxide particles, resulting in a small amount of quinaldine blue oxidation in the absence of ligand.

The activity of the copper(II)-picolinic acid system as a function of the ratio of ligand to copper(II), with constant amount of copper(II), is shown in Figure 3-2. The most active species is formed at a 1:1 ratio of copper to ligand. Examination of the stability constants involved shows that the formation of the 1:1 complex, $\text{Cu}(\text{PA})^+$, is the dominant species under these conditions.⁴⁵

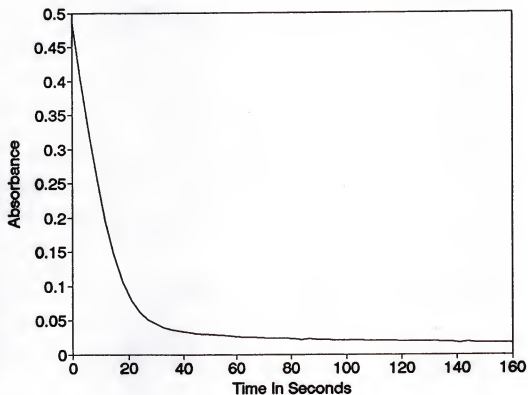


Figure 3-1: Oxidation of quinaldine blue with hydrogen peroxide catalyzed by copper(II) chloride + picolinic acid. $[\text{H}_2\text{O}_2] = 2.9 \times 10^{-3} \text{ M}$, $[\text{CuCl}_2] = 2.9 \times 10^{-3} \text{ M}$.

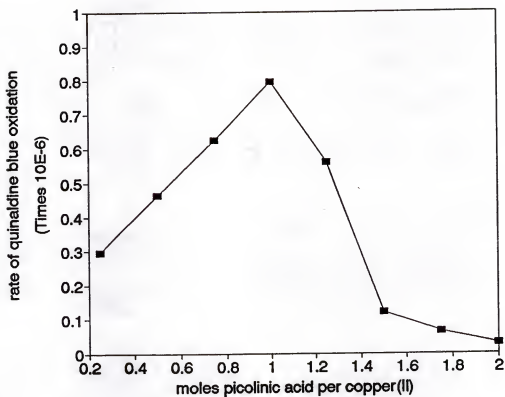


Figure 3-2: The effect of ligand:metal ratio on the rate of quinaldine blue oxidation. $[\text{Cu}^{2+}] = 2.9 \times 10^{-3} \text{ M}$, $[\text{H}_2\text{O}_2] = 5.7 \times 10^{-3} \text{ M}$. All rates are expressed in terms of (moles quinaldine blue) $(\text{liter})^{-1}(\text{second})^{-1}$.

The oxidation of quinaldine blue with different concentrations of the $\text{Cu}(\text{PA})^+$ complex, peroxide, and quinaldine blue were studied. Table 3-1 (runs 1-8) gives the rate of quinaldine blue oxidation when the copper concentration in the cell is held constant at $2.9 \times 10^{-5} \text{ M}$ and the peroxide concentration is varied from $5.7 \times 10^{-4} \text{ M}$ to $2.9 \times 10^{-2} \text{ M}$. The rate of oxidation is zero order in hydrogen peroxide for the range of peroxide concentrations studied. Rate measurements on replicate runs are reproducible, varying a maximum of 5%. Studies were then performed at constant peroxide concentration, 0.029 M, while the $\text{Cu}(\text{PA})^+$ concentration was varied. These results are shown in Table 3-1, runs 9-14. A $\ln(\text{initial concentration})$ versus $\ln(\text{rate})$ plot gave a reaction order in the copper complex of one. The order with respect to substrate is zero, as determined from runs 13, 15, and 16. A mechanism consistent with these observations will be presented in the discussion section of this chapter.

Effect of pH on Quinaldine Blue Oxidation Rate

The rate of quinaldine blue oxidation catalyzed by the copper(II)-picolinic acid system was measured at different pH levels. The copper complex concentration was held constant at $2.9 \times 10^{-5} \text{ M}$, and the peroxide concentration was $2.9 \times 10^{-3} \text{ M}$. The pH was adjusted by the addition of small amounts of concentrated KOH solution to a solution of the catalyst and tetraborate. Figure 3-3 shows the rate dependence on pH. At pH levels below 8.0, the rate of quinaldine blue oxidation is negligible. As the pH increases, the rate of reaction increases until the pH approaches 10.0, at which point, the rate as a function of pH levels off. The final pH of the reaction solution was not significantly different from the original pH.

Table 3-1: Dependence of quinaldine blue oxidation rate on peroxide, Cu(PA)^+ concentration, and substrate concentration.

Run	$[\text{H}_2\text{O}_2]^a$	[Quin. Blue]	$[\text{Cu(PA)}^+]$	Rate ^b
1	5.70×10^{-4}	3.0×10^{-5}	2.9×10^{-5}	8.4×10^{-7}
2	5.70×10^{-4}	"	"	8.3×10^{-7}
3	2.86×10^{-3}	"	"	7.9×10^{-7}
4	2.86×10^{-3}	"	"	7.8×10^{-7}
5	8.59×10^{-3}	"	"	7.9×10^{-7}
6	8.59×10^{-3}	"	"	7.6×10^{-7}
7	1.72×10^{-2}	"	"	7.1×10^{-7}
8	2.86×10^{-2}	"	"	7.3×10^{-7}
9	2.86×10^{-2}	"	1.4×10^{-6}	9.3×10^{-9}
10	"	"	1.8×10^{-6}	2.0×10^{-8}
11	"	"	2.3×10^{-6}	5.4×10^{-8}
12	"	"	1.1×10^{-5}	3.2×10^{-7}
13	"	"	2.9×10^{-5}	7.3×10^{-7}
14	"	"	8.6×10^{-5}	9.2×10^{-7}
15	"	2.0×10^{-5}	2.9×10^{-5}	7.6×10^{-7}
16	"	1.0×10^{-5}	"	7.5×10^{-7}

^a All concentrations are in moles per liter

^b Rates are expressed in terms of (moles quinaldine blue)(liter)⁻¹(second)⁻¹.

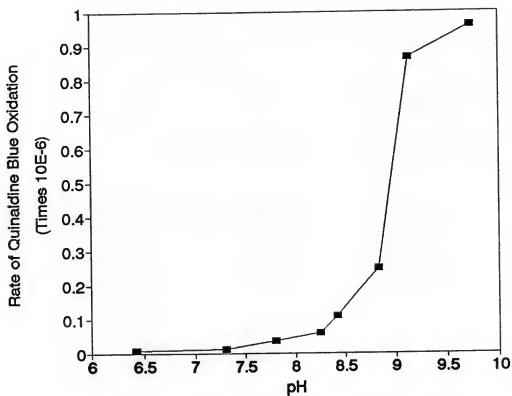


Figure 3-3: The effect of pH on the rate of quinaldine blue oxidation. The catalyst concentration used is 2.9×10^{-3} M Cu^{2+} /PA, the peroxide concentration is 5.7×10^{-3} M. Rates are expressed in units of $(\text{moles quinaldine blue})(\text{liter})^{-1}(\text{second})^{-1}$.

Peroxide Activation by Copper(II) Complexes of Anionic Bidentate Ligands

A set of experiments were performed with acetylacetone (AcAc), glycine (GLY), alanine (ALA), and leucine (LEU) as ligands. Glycine, alanine, and leucine have carboxyl and nitrogen donor groups. Acetylacetone provides a different anionic, bidentate ligand system consisting of oxygen donors. The concentration of catalyst was 2.8×10^{-5} M in all of the experiments, and the concentration of peroxide was 2.8×10^{-2} M. In these studies, the rate of quinaldine blue oxidation was studied with both 1:1 and 2:1 ratios of ligand to copper(II). The initial rates of oxidation for the copper complexes of anionic bidentate ligands are shown in Table 3-2, as runs 1-14.

All complexes of the bidentate anionic ligands studied catalyze the oxidation of quinaldine blue using hydrogen peroxide as the oxidizing agent. The amino acids exhibited a fairly broad range of activity, with glycine being the least active and leucine being the most active at a 1:1 ratio of ligand to metal. The copper(II) complex of acetylacetone showed the best activity, giving a rate of quinaldine blue oxidation 15-20% faster than the copper(II) leucine complex. As in the picolinic acid system, all of these complexes exhibited a sharp decrease in activity when the ratio of ligand to metal was raised above a 1:1 mole ratio.

Peroxide Activation by Copper(II) Complexes of Tridentate Anionic Ligands

Two tridentate anionic ligands, dipicolinic acid (DPA) and iminodiacetic acid (IDA) were examined. The results of this study are shown in Table 3-2, as runs 11-14. The copper(II) complexes of tridentate anionic ligands at a 1:1 mole ratio are much poorer

Table 3-2: Rate of quinaldine blue oxidation for copper(II) complexes of anionic bidentate (runs 1-10), and anionic tridentate (runs 11-14) ligands.

Run #	Catalyst ^a	Rate Of Substrate Oxidation ($\times 10^{-7}$) ^b
1	Cu ^{II} / 1 PA	7.9
2	Cu ^{II} / 2 PA	0.21
3	Cu ^{II} / 1 AcAc	11.1
4	Cu ^{II} / 2 AcAc	1.8
5	Cu ^{II} / 1 GLY	4.7
6	Cu ^{II} / 2 GLY	1.9
7	Cu ^{II} / 1 ALA	5.9
8	Cu ^{II} / 2 ALA	3.2
9	Cu ^{II} / 1 LEU	8.8
10	Cu ^{II} / 2 LEU	2.6
11	Cu ^{II} / 1 DPA	1.5
12	Cu ^{II} / 2 DPA	0.014
13	Cu ^{II} / 1 IDA	2.9
14	Cu ^{II} / 2 IDA	0.17

^aThe concentration of copper(II) used was 2.8×10^{-5} M and the concentration of hydrogen peroxide was 2.8×10^{-3} M. All reaction solutions were buffered at pH=9.1.

PA=picolinic acid, AcAc=acetylacetone, GLY= glycine, ALA= alanine, LEU= leucine, DPA= dipicolinic acid, IDA= iminodiacetic acid.

^bRates are in units of (moles) (liter)⁻¹ (second)⁻¹.

catalysts for oxidation by hydrogen peroxide than the copper(II) complexes of the bidentate anionic ligands. At 2:1 ligand to metal ratios the tridentate anionic ligands show little activity for peroxide activation. The reduction in activity for complexes of anionic tridentate ligands, relative to the anionic bidentate systems, is interesting. This shows that either a positively charged complex is needed, or two coordination sites in the equatorial positions must be occupied by water to generate an effective copper(II) catalyst for peroxide activation.

Peroxide Activation by Copper(II) Complexes of Neutral Bidentate Ligands

Copper(II) complexes of the bidentate neutral ligands ethylenediamine (EN), N,N,N',N'-tetramethylethylenediamine (TMED), 2,9-dimethyl-1,10-phenanthroline (DMP), and 2,2'-bipyridylamine (BPA) were examined as possible catalysts for activation of hydrogen peroxide. Table 3-3, runs 1-10, demonstrate that the copper(II) complexes of bidentate neutral ligands are very effective as catalysts for the oxidation of quinaldine blue with hydrogen peroxide. The copper(II) complex of 2,2'-bipyridylamine, in particular, was shown to have exceptional activity.

The variation in the rates from catalysis with the copper(II) complexes of ethylenediamine (EN) and N,N,N',N'-tetramethylethylenediamine (TMED) in the presence of excess ligand is interesting. In the case of EN the activity is reduced by a factor of 50 with the addition of one equivalent of excess ligand. However, the activity of the TMED complex was decreased only slightly by the presence of a four-fold excess of ligand. Sterically hindering ligands that decrease the equilibrium constant for binding a

Table 3-3: Rate of quinaldine blue oxidation for copper(II) complexes of neutral bidentate (runs 1-10), and neutral multidentate (runs 11-16) ligands.

Run #	Catalyst ^a	Rate Of Substrate Oxidation ($\times 10^{-7}$) ^b
1	Cu ^{II} / 1 EN	5.2
2	Cu ^{II} / 2 EN	0.10
3	Cu ^{II} / 1 TMED	6.4
4	Cu ^{II} / 2 TMED	5.9
5	Cu ^{II} / 4 TMED	3.9
6	Cu ^{II} / 1 DMP	10.2
7	Cu ^{II} / 2 DMP	0.0
8	Cu ^{II} / 1 BPA	35.1
9	Cu ^{II} / 2 BPA	23.4
10	Cu ^{II} / 5 BPA	12.6
11	Cu ^{II} / 1 TREN	0.0
12	Cu ^{II} / 2 TREN	0.0
13	Cu ^{II} / 1 IBPA	0.0
14	Cu ^{II} / 2 IBPA	0.0
15	Cu ^{II} / 1 TERPY	0.06
16	Cu ^{II} / 2 TERPY	0.05

^aConcentrations are in moles per liter. EN= ethylenediamine, TMED= tetramethylenediamine, DMP= 2,9-dimethyl-1,10-phenanthroline, BPA= bipyridylamine, TREN = tris(2-aminoethyl)amine, IBPA= iminobis(propylamine) TERPY= terpyridine

^bRates are in units of (moles) (liter)⁻¹ (second)⁻¹.

second bidentate ligand produce copper complexes which function in the presence of excess ligand. Examination of the formation constants for the 1:1 and 2:1 complexes of both EN and TMED show that, indeed, the formation of the 2:1 complex is much less favorable with TMED.⁴⁵

Peroxide Activation With Copper(II) Complexes of Neutral Multidentate Ligands

To complete this study, several copper(II) complexes with neutral tri- and tetradentate ligands were investigated as possible catalysts. Table 3-3, runs 11-16, show the results with copper(II) complexes of Tris(2-aminoethyl)amine (TREN), 3,3'-iminobis(propylamine) (IBPA), and 2,2':6,6''-terpyridine (TERPY). The conditions and peroxide concentrations were the same as above. Since the copper(II) complexes of tri- and tetradentate neutral ligands result in poor or inactive catalysts, we can conclude that having two equatorial coordination positions occupied with easily displaced solvent, and not the complex charge, is the necessary condition for the formation of the active catalytic species.

Rate Studies

In order to examine the mechanism, several of the complexes were selected for further kinetic examination. The copper(II)/ leucine catalyst was selected because it gave the best performance for peroxide activation among the amino acids. The copper(II)/ acetylacetone complex was selected because it gave the best performance of the anionic ligands. The copper(II)/ 2,2'-bipyridylamine complex was selected because it gave the best overall peroxide activation. The copper(II)/ N,N,N',N'-tetramethylethylenediamine

complex was selected to determine the influence of steric effects on the reaction mechanism.

The copper(II) complexes of all these ligands give a first order dependence on catalyst concentration similar to that observed for the copper(II) complex of picolinic acid. The results for LEU and AcAc are shown in Table 3-4. The other ligands show similar behavior. The copper(II)-leucine complex, like the copper(II) picolinic acid complex, showed zero order behavior based on peroxide. However, the copper(II) complexes of the three other ligands selected showed significant deviations from zero order behavior based on peroxide. Tables 3-5 shows the rates of quinaldine blue oxidation for these complexes as the peroxide concentration is changed. The catalyst concentration is kept constant at 2.8×10^{-5} M for the copper(II)-AcAc and copper(II)-TMED complexes and, because of its increased activity, at 2.8×10^{-6} M for the copper(II)- BPA complex. For quinaldine blue oxidations catalyzed by copper(II)- picolinic acid and copper(II)-leucine, the oxidation rates were 7.9×10^{-7} and 8.8×10^{-7} (moles) (liter)⁻¹ (second)⁻¹ respectively. These rates did not change significantly with changes in peroxide concentration.

The Proposed Mechanism and Rate Law

A wide variety of copper(II) complexes are shown to be effective activators for hydrogen peroxide in this chapter. The reactivity of these complexes are inhibited dramatically when the ligand to metal ratio is higher than 1:1. Tri- and tetradentate ligands are much less active than the bidentate ligands. These results suggest that a significant concentration of copper(II) complex with two available coordination positions in the XY

Table 3-4: Rate of oxidation of quinaldine blue for various concentrations of copper(II) complexes of LEU and AcAc. Peroxide concentration was held constant at 2.8×10^{-2} M

Run #	Ligand	Complex Concentration ^a	Rate Of Quinaldine Blue Oxidation ($\times 10^{-3}$) ^b
1	LEU	2.9×10^{-5}	8.8
2	LEU	2.3×10^{-5}	6.8
4	LEU	1.1×10^{-5}	4.4
5	LEU	5.7×10^{-6}	1.7
6	LEU	2.3×10^{-6}	0.67
7	AcAc	2.9×10^{-5}	11.1
8	AcAc	1.7×10^{-5}	8.5
9	AcAc	1.1×10^{-5}	5.9
10	AcAc	5.7×10^{-6}	2.2
11	AcAc	2.3×10^{-6}	0.65

^aConcentrations are in moles per liter.

^bRates are in units of (moles) (liter)⁻¹ (second)⁻¹.

Table 3-5: Rate of quinaldine blue oxidation for various peroxide concentrations with 2.8×10^{-6} M of copper(II)- BPA (runs 1-4), 2.8×10^{-5} M copper-AcAc (runs 5-10), and 2.8×10^{-5} M copper(II)-TMED (runs 11-21).

Run #	Ligand	Peroxide Concentration ^a	Rate of Quinaldine Blue Oxidation ($\times 10^{-3}$) ^b
1	BPA	0.0286	3.66
2	BPA	0.00916	2.29
3	BPA	0.00466	1.55
4	BPA	0.000573	0.226
5	AcAc	0.0286	11.2
6	AcAc	0.00916	11.1
7	AcAc	0.00466	9.8
8	AcAc	0.00115	8.9
9	AcAc	0.000573	5.7
10	AcAc	0.000286	4.6
11	TMED	0.0286	5.8
12	TMED	0.0286	5.0
13	TMED	0.00916	4.5
14	TMED	0.00916	4.4
15	TMED	0.00466	3.0
16	TMED	0.00466	3.2
17	TMED	0.00115	1.6
18	TMED	0.000573	1.0
19	TMED	0.000573	0.97
20	TMED	0.000286	0.40
21	TMED	0.000286	0.383

^aConcentrations are in moles per liter.

^bRates are in units of (moles) (liter)⁻¹ (second)⁻¹.

plane (i.e. occupied only by solvent) is a requisite for an active catalyst for oxidations using hydrogen peroxide.

The mechanism for activation of hydrogen peroxide by copper(II) complexes must account for the following observations:

- 1) The order with respect to quinaldine blue is zero.
- 2) All reactions are first order in the copper complex.
- 3) The addition of ligand above a 1:1 mole ratio of ligand to copper(II) decreases activity, and the tri- or tetradentate ligands also tend to give inactive complexes.
- 4) The reaction rate is pH dependent.
- 5) The order in peroxide concentration is zero for PA and LEU, but nonzero for AcAc, TMED, and BPA.

A mechanism consistent with these observations is shown in Figure 3-4.

The first step is the reversible dissociation of one coordinated water from a tetragonal, six coordinate copper(II) complex. This process is reported to be reasonably facile,²⁴ as the Jahn-Teller effect causes the axial-bound waters to be weakly coordinated. The next step is coordination of the hydroperoxide anion (O_2H^-) to produce the peroxo or hydroperoxo complex. To obtain effective catalysts, the coordinated peroxide must occupy a stronger binding equatorial position, *trans*- to the ligand. Peroxide binding to the equatorial positions is the key to understanding the effect of excess ligand and the low reactivity of the tri- and tetra-dentate systems. Once formed, this copper-hydroperoxide species reacts extremely rapidly with the substrate. As a result, the rate of oxidation is determined by the

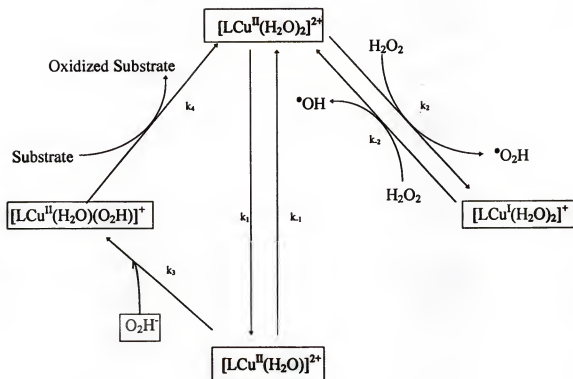


Figure 3-4: The proposed mechanism for oxidations with copper(II) complexes. L = ligand.

rate of formation of the copper-hydroperoxide complex, resulting in a zero order substrate dependence.

Assuming that the rate of formation of the copper-hydroperoxide complex is rate limiting, and is followed by rapid oxidation of quinaldine blue, the rate of oxidation catalyzed by the copper(II) complex is given by

$$v_{\text{ox}} = d [\text{LCu}^{\text{II}}(\text{H}_2\text{O})(\text{O}_2\text{H})] / dt = k_3 [\text{LCu}^{\text{II}}(\text{H}_2\text{O})] [\text{O}_2\text{H}^+] \quad (3-1)$$

(where the subscripts on the rate constants refer to the steps of the proposed mechanism in Figure 3-4.)

A steady-state approximation for the $[\text{LCu}^{\text{II}}(\text{H}_2\text{O})]$ concentration leads to the following expression:

$$[\text{LCu}^{\text{II}}(\text{H}_2\text{O})] = \frac{k_1 [\text{LCu}^{\text{II}}(\text{H}_2\text{O})_2]}{k_{-1} + k_3 [\text{O}_2\text{H}^+]} \quad (3-2)$$

The concentration of the hydroperoxide anion is directly proportional to peroxide concentration and pH; $[\text{O}_2\text{H}^+] = K_a [\text{H}^+] [\text{H}_2\text{O}_2]$. Substituting Equation (3-2) into Equation (3-1) gives the rate of oxidation as

$$\text{Reaction Rate} = \frac{k_1 k_3 [\text{LCu}^{\text{II}}(\text{H}_2\text{O})_2] [\text{O}_2\text{H}^+]}{k_{-1} + k_3 [\text{O}_2\text{H}^+]} \quad (3-3)$$

Equation (3-3) can be rearranged to

$$\text{Reaction Rate} = \frac{k_1[\text{LCu}^{\text{II}}(\text{H}_2\text{O})_2] [\text{O}_2\text{H}^-]}{(k_{-1} / k_3) + [\text{O}_2\text{H}^-]} \quad (3-4)$$

In addition, if we derived the rate law by using two consecutive steady-state approximations for both $[\text{LCu}^{\text{II}}(\text{H}_2\text{O})]^{2+}$ and $[\text{LCu}^{\text{II}}(\text{O}_2\text{H})]^+$, we obtain the same rate law as in Equation (3-4). The only requirement for this to be valid is that the rate for substrate oxidation be equal to or greater than the rate of copper(II) hydroperoxide complex formation.

Comparison of the Proposed Mechanism to Observed Reactivity

The experimental observations support the above mechanism, and suggest that other possibilities are less reasonable. First, the active species does not seem to be a simple dissociated hydroxyl radical produced by peroxide decomposition, as in Fenton chemistry. While a pathway does exist for this, as shown in the mechanism (the k_2 pathway), this reaction cannot account for the dramatic decrease in reactivity seen for oxidations catalyzed by complexes of tridentate ligands. A second possible mechanism involves a high oxidation state of copper as the active oxidant. While some copper(II) complexes have been shown to be strong enough oxidants to react with amine-containing buffers,^{43,44} no oxidation reaction occurs between copper(II) and quinaldine blue in the absence of hydrogen peroxide. Copper(III) species are known in aqueous solutions.^{46,47} However, a

Class V reaction mechanism involving copper(III) cannot explain the need for two available equatorial binding sites. A mechanism involving a coordinated peroxide explains both the trends in reactivity of the mono- and dipositively charged copper(II) complexes, and the reduction in reactivity that occurs in the presence of excess ligand.

The decrease in reactivity with excess ligand can be understood in terms of copper(II) coordination chemistry. The dissociation of water occurs from the axial positions, as these bonds are weakened relative to the equatorial positions by Jahn-Teller distortion. Once the five coordinate copper complex is formed, the attack by O_2H^- occurs so as to coordinate the O_2H^- in the strong binding equatorial position. The strongest binding of hydroperoxide anion occurs when it is bound to the same $d_{x^2-y^2}$ orbital that is involved in ligand coordination. Coordination of O_2H^- to the equatorial position is important because use of this orbital leads to a stronger acceptor than the axial position. Strong Lewis acidity activates hydrogen peroxide in Class IVb mechanisms. When the 2:1 ligand to copper(II) complex is formed, the reactivity decreases because there are no longer any strong-binding equatorial positions available to bind the hydroperoxide anion.

Our experiments show that it is necessary to have two equatorial coordination sites occupied by easily displaced solvent. This is demonstrated by the large decrease in reactivity seen with complexes of tri- and tetra-dentate ligands, as compared to the bidentate ligands. There are several possible reasons for this. The most straightforward is that it is necessary to have two coordination sites to bind the peroxide, in which case the complex shown in Figure 3-5a is formed. Complexes of copper(II) dimers have been

shown to bind O_2^{2-} in a similar manner.^{33c,35b-c,36b,37a} Many peroxo complexes of other metals are known⁴⁸ and several are useful oxidants and oxidation catalysts.⁴⁹

Another possibility is that the metal-peroxo complex is stabilized by a hydrogen bonding interaction between bound hydroperoxide and an equatorial water. A similar interaction has been used to explain the stability of a vanadium-peroxo complex in aqueous solution.¹⁰ This interaction can only occur when one bidentate ligand is coordinated to the copper center, as shown in Figure 3-5. When a tri- or tetradentate ligand is coordinated to the copper(II) complex, or a 2:1 complex of the bidentate ligand is formed, stabilization of the hydroperoxide anion through hydrogen bonding does not occur.

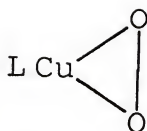
For an equatorially bound copper(II) hydroperoxide complex, some radical character is expected in the bound hydroperoxide:



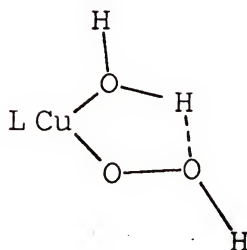
The degree of radical character is likely to be somewhere between the two extremes listed above, and is expected to vary with the ligand coordinated to the copper(II) center.

Comparison of Derived Rate Law To Observed Kinetics

Our proposed mechanism (Figure 3-4) leads to a rate law, Equation (3-4), that explains our kinetic data. The requirement that our mechanism gives zero order kinetics for quinaldine blue oxidation is satisfied with the assumption that the copper(II) hydroperoxide species will react very fast with the quinaldine blue. This is reasonable, as



A



B

Figures 3-5: Proposed structures for: a) the μ^2 bound peroxide and b) the hydrogen-bond stabilized copper-hydroperoxide complex.

oxone® and sodium hypochlorite oxidize quinaldine blue too rapidly to accurately determine reaction rates with the procedures used here.

The rate of oxidation is predicted, by the derived rate law, to be first order in copper(II) complex. This is in keeping with our experimental evidence. In all cases, a first order dependence of reaction rate on copper(II) concentration was observed. The dependence of oxidation rate on hydrogen peroxide concentration and pH are more complex. A zero order dependence of the rate on peroxide concentration was observed for copper(II) complexes of picolinic acid (PA) and leucine (LEU). However, the copper(II) complexes of acetylacetone (AcAc), N,N,N',N'-tetramethylethylenediamine (TMED), and bipyridylamine (BPA) all showed significant deviations from zero order kinetics.

Figure 3-6 shows how the rate of quinaldine blue oxidation changes with peroxide concentration for copper(II) complexes of AcAc, TMED, and BPA.

While these results are not in agreement with the zero-order dependence seen for copper(II) complexes of picolinic acid or leucine, the rate law derived from the proposed mechanism (Equation 3-4) can be used to explain these differing orders. If we define V_{\max} as $k_1[\text{LCu}^{\text{II}}(\text{H}_2\text{O})_2]$ and K_m as k_{-1} / k_3 we obtain the following expression:

$$\text{Reaction Rate} = \frac{V_{\max}[\text{O}_2\text{H}]}{K_m + [\text{O}_2\text{H}]} \quad (3-5)$$

Equation (3-5), obtained from our derived rate law, is in the same form as the Michaelis-Menten equation, often used to describe reaction rates in enzyme systems.⁵⁰

Systems following Michaelis-Menten type kinetics will give Lineweaver-Burk plots of $(\text{rate})^{-1}$ versus $[\text{HO}_2^-]^{-1}$ that are linear. Figures 3-7, 3-8, and 3-9 show the Lineweaver-Burk plots for the Cu-AcAc, Cu-TMED, and Cu-BPA systems.

The linearity of these plots shows that our systems follow the kinetics predicted by the derived rate law, Equation 3-5. In these plots, the slope is equal to K_m/V_{max} and the y-intercept is equal to $(V_{\text{max}})^{-1}$. Table 3-6 shows the values for these kinetic parameters as determined from our data. For the copper(II) complexes of picolinic acid and leucine V_{max} is the observed rate of reaction, as peroxide concentrations low enough to cause deviation from zero order kinetics were not examined. Since K_m must clearly be lower than $[\text{HO}_2^-]$ to give zero-order kinetics in peroxide, based on Equation (3-5), maximum possible K_m values for these catalysts are reported based on the lowest hydroperoxide anion concentration studied.

Interestingly, dipositively charged copper(II) complexes (neutral ligands) have significantly higher values of K_m for peroxide activation. As K_m is equal to k_{-1}/k_3 in the derived rate law, this implies that coordination of water to the dissociated copper(II) complex ($[\text{LCu}(\text{H}_2\text{O})]$), rather than coordination of the hydroperoxide anion, is more favorable for the more positively charged copper complexes. In view of the complex enthalpic and entropic contributions to the coordination of these species, we cannot draw any conclusions on the reason for the trends observed in K_m or V_{max} .

The rates of oxidation are dependent upon the concentration of the hydroperoxide anion, rather than hydrogen peroxide. The effect of pH changes on reaction rates, shown in Figure 3-3 for the copper(II) complex of picolinic acid, can therefore be explained

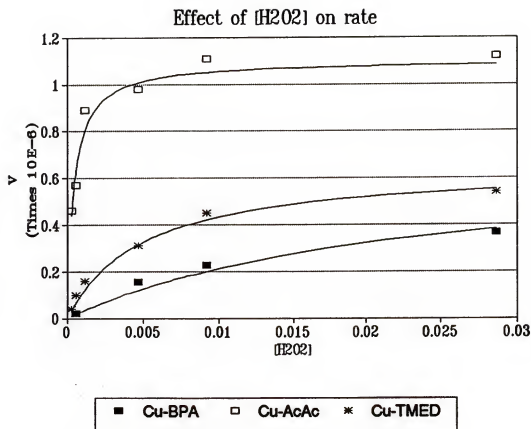


Figure 3-6: The rate of oxidation as a function of peroxide concentration for the copper(II) complexes of AcAc, TMED, and BPA

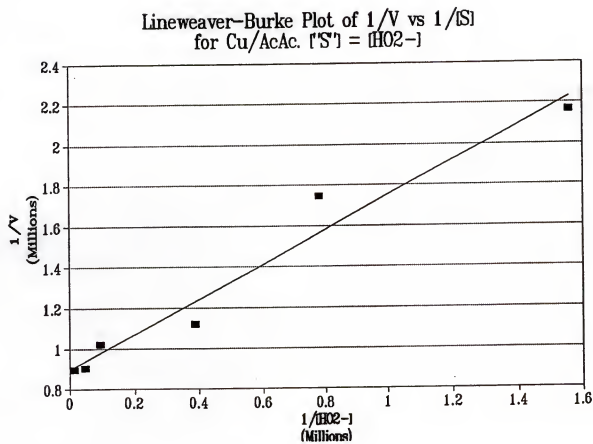


Figure 3-7: Lineweaver-Burk plot of $1/\text{rate}$ vs. $1/[H_2O_2]$ for the copper-AcAc complex

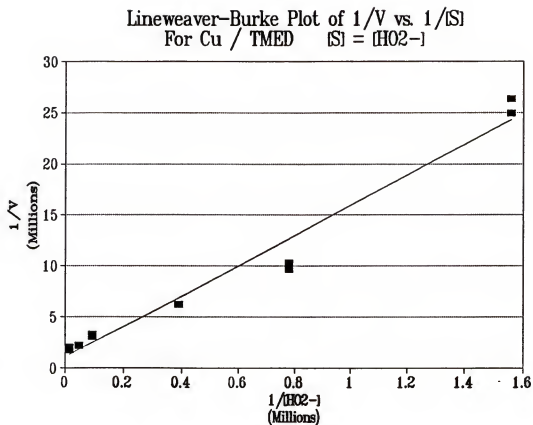


Figure 3-8: Lineweaver-Burk plot of $1/\text{rate}$ vs $1/[HO_2^-]$ for the copper-TMED complex

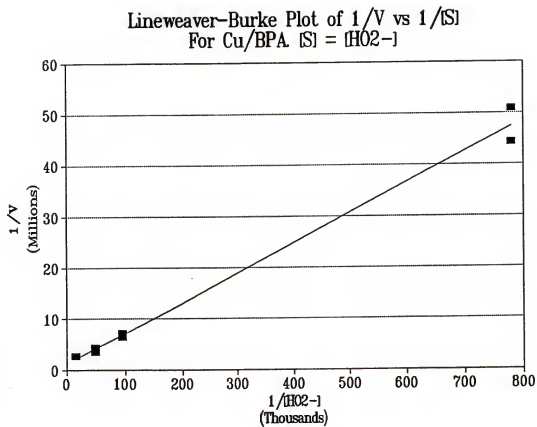


Figure 3-9: Lineweaver-Burk plot of $1/\text{rate}$ vs. $1/[HO_2^-]$ for the copper-BPA complex

Table 3-6: Values for V_{\max} and K_m as determined for the copper(II) complexes of various ligands.

Ligand	V_{\max}^a	K_m
PA	7.9×10^{-7}	$< 8 \times 10^{-7}$
LEU	8.8×10^{-7}	$< 8 \times 10^{-7}$
AcAc	1.1×10^{-6}	9.4×10^{-7}
TMED	9.1×10^{-7}	1.4×10^{-5}
BPA	8.1×10^{-6}	4.8×10^{-5}

^aThe V_{\max} is expressed for a complex concentration of 2.8×10^{-5} M.

within the context of our mechanism and derived rate law. The concentration of hydroperoxide anion is given by

$$[\text{HO}_2^-] = K_a [\text{H}_2\text{O}_2] [\text{H}^+]^{-1} \quad (3-6)$$

$$(K_a = 1.78 \times 10^{-12})$$

At high pH the concentration of hydroperoxide anion will be high enough to give zero-order kinetics, where the observed rate is equal to V_{max} . As the pH drops between 9.5 and 9 no significant decrease in rate is seen from the resultant decrease in hydroperoxide anion concentration. This is because there is still a high enough concentration of hydroperoxide to give the observed rate as V_{max} . However, as the pH drops much below 9, the concentration of hydroperoxide anion decreases enough to see deviation from zero-order kinetics similar to that seen for the copper(II) complexes of AcAc, TMED, and BPA. This gives rise to a dependence of rate upon the decreasing hydroperoxide anion concentration.

Conclusions

We have found a series of copper(II) complexes that are able to activate hydrogen peroxide for oxidation in basic aqueous solution. In all cases, increasing the amount of ligand above a 1:1 ratio to copper(II) decreases the rate of peroxide activation, in some cases dramatically. Complexes of tri- and tetra- dentate ligands are generally inactive. A mechanism (Figure 3-4) is proposed which involves the dissociation of coordinated water from the axial position, followed by nucleophilic attack by a hydroperoxide anion, to form an equatorially bound copper(II)-hydroperoxide complex. The more strongly coordinating

equatorial position provides the needed Lewis acidity to activate bound hydroperoxide for substrate oxidation. Several theories are examined on why two equatorial coordination sites containing easily displaced solvent are necessary for peroxide activation with these complexes. One possibility is that the peroxide occupies two coordination sites, as in Figure 3-5b. Another possibility is that the coordinated hydroperoxide is stabilized by hydrogen-bonding interaction with a coordinated water, as in Figure 3-5a. A first order dependence of rate on catalyst concentration is observed, which is shown to agree with the rate law derived from our mechanism (Equation 3-4). The observed zero order dependence of oxidation rate on substrate concentration is also explained within the context of the proposed mechanism

The observation of zero-order dependence of rate on hydrogen peroxide concentration for PA and LEU and the nonzero-order rate dependence for AcAc, TMED, and BPA are also explained. This is done by re-writing Equation (3-4), the derived rate law, in the form of the Michaelis-Menten expression. This expression predicts under which conditions the rate of reaction is equal to V_{\max} , where the zero-order rate dependence on peroxide concentration occurs. This also explains the observed dependence of reaction rate upon pH for oxidations catalyzed by the copper(II)-picolinic acid complex. As the pH decreases the concentration of hydroperoxide anion also is decreased. When the pH drops below that needed for sufficient concentration of hydroperoxide anion to give the observed rate as V_{\max} , a decreased rate is observed.

The mechanism offered for these systems can be generalized. In order to activate hydrogen peroxide by coordination of the peroxide to a metal center, the complex used

must be capable of binding O_2H^- to a strongly acidic coordination position. The stability constants for successive ligand binding can be employed to select metal complexes that have the potential to bind and activate O_2H^- . The sequence of formation constants must allow the existence of aquo complexes with which O_2H^- can react by displacing water from strong binding metal orbitals. For copper(II), the 2:1 ($\text{Cu}(\text{L})_2$) formation constant must be low enough relative to the 1:1 ($\text{Cu}(\text{L})$) to permit substantial quantities of the 1:1 complex to exist in solution. For metal ions with fewer d-electrons, strong axial coordination positions exist and if 2:1 bidentate ligand complexes are prepared they could lead to strong binding of O_2H^- .

CHAPTER 4

ACTIVATION OF HYDROGEN PEROXIDE FOR OXIDATION WITH VANADIUM-PEROXO COMPLEXES

Introduction

Using a transition metal complex to activate hydrogen peroxide through electron-transfer (Class III, IVa and V mechanisms) often catalyzes peroxide decomposition. The two-electron transfer case (Class III), and the conditions under which it leads to decomposition, were discussed in chapter 2. One-electron activation of hydrogen peroxide also catalyzes decomposition (Class IVa), and while direct activation (see p. 6) is possible, the goal of efficient peroxide use cannot be met with this type of mechanism.

Catalysts which perform oxidations by Class IVb mechanisms, where the active oxidant is a metal peroxo or hydroperoxo complex, have the potential to avoid peroxide decomposition. This is because the pathway to substrate oxidation does not necessarily involve electron-transfer between the transition metal complex and hydrogen peroxide. In the oxidations discussed in this chapter, the metal-peroxo species is formed, or regenerated, from the reaction of a metal-oxo complex with hydrogen peroxide, as shown in Figure 4-1. In the process of oxygen atom transfer from hydrogen peroxide to the transition metal complex, the oxidation state of the metal center does not change, thus limiting the pathways available for decomposition. Therefore, oxidation through this mechanism may be able to activate hydrogen peroxide efficiently for oxidation.

Catalytic oxidation of organic substrates with d^0 metal-peroxo complexes has been an area of growing interest.^{51,52} In particular, the use of vanadium-peroxo complexes as catalysts for peroxide activation has been the subject of many publications over the last few years.⁵³⁻⁵⁵ A recent paper showed significant correlation between the one-electron reduction potential and oxygen-oxygen bond strength for a wide variety of metal peroxo complexes.⁵⁶ It was shown, for complexes with the same transition metal center, those complexes with stronger O-O peroxo bonds have lower one-electron reduction potentials than complexes with weaker O-O bonds.

One proposed mechanism for oxidation using metal peroxo complexes involves the cleavage of a metal-peroxide bond to form a bound peroxide radical. In the process of the intramolecular electron transfer, the metal center is reduced.^{53b} Other mechanisms have been proposed which involve the formation of a bound oxo radical from a one electron reduction of the entire complex (requiring a reductant in solution), followed by cleavage of the peroxide to form the active oxidizing species.^{54b,e} In either case, a reduction of the vanadium complex through an intramolecular electron transfer (Figure 4-2 a) or through electron transfer to the complex (Figure 4-2 b) is necessary to perform oxidation.

The complexes known to perform catalytic oxidation include $V(O)(AcAc)_3$,⁵⁵ $V(O)(O_2)(PA)_3$,^{54c,e,57} and $V(O)(i-PrO)_3$.^{54f} In this chapter, we compare the ability of another vanadium peroxo complex, $[V(bipy)_2(O_2)](ClO_4)_2$, to act as a catalyst for peroxide activation to the $V(O)(AcAc)_3$ and $V(O)(O_2)(PA)_3$ systems. The bis(bipyridine) complex was previously prepared and shown to have an unusually short O-O peroxo bond distance.⁵⁸ However, no experiments have been performed to determine the possible

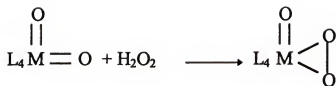


Figure 4-1: Formation of the metal-peroxo complex

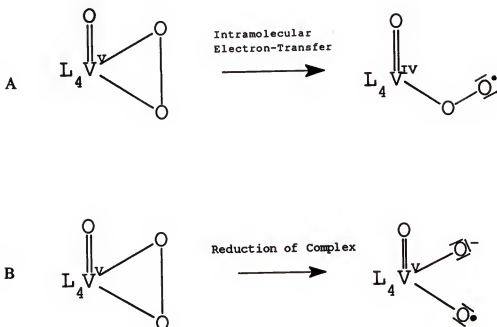


Figure 4-2: Generation of the active radical species from the vanadium peroxo complexes. (a) is for the mechanism proposed by Mimoun, (b) is for the mechanism proposed by Di Furia.

usefulness of this complex as a catalyst for peroxide activation. Both mechanisms for oxidation by vanadium peroxo complexes (Figure 4-2) involve a one-electron transfer, either from bound peroxide or from a reductant in solution, to the vanadium. Therefore, the easier it is to reduce the vanadium center, the more thermodynamically favorable the pathway to substrate oxidation will be. The one-electron reduction potential of d^0 metal-peroxo complexes⁵⁶ was found to be directly related to the strength of the peroxide bond. Vanadium complexes having shorter, stronger O-O bonds had significantly lower reduction potentials. The unusually short O-O bond distance in the vanadium-bipy complex (1.24 Å) compared to the other vanadium peroxo complexes (>1.4 Å) should give rise to much lower reduction potentials, and result in a superior catalyst for oxidations.

In this chapter, the catalytic oxidation of benzene and cyclohexane are examined, using hydrogen peroxide and the vanadium peroxo complexes mentioned above. To compare the effectiveness of these vanadium complexes as peroxide activators, we observed the increase in concentration of the oxidized products by gas chromatography. For benzene oxidation, the increase in phenol concentration was observed. For cyclohexane oxidation, the increase in both cyclohexanol and cyclohexanone concentration was measured. While in both cases there are other products formed, the research in this chapter focuses only on those products listed above as a means of evaluating the relative rates of oxidation for the different catalyst systems.

Experimental

Materials

V_2O_5 , $VO(AcAc)_2$ (AcAc=acetylacetone), dipicolinic acid (DPA), picolinic acid (PA), Cyclohexanol, D_2O (99.9% atom D), cyclohexanone, 2,2'-bipyridine (bipy), and benzene were all used as received from Aldrich. KCl, 30% H_2O_2 , phenol, CH_3CN , and cyclohexane were all used as received from Fisher.

Synthesis

$K[VO_2(DPA)]$. This complex was synthesized by the method reported in reference 59. 2.25 g of V_2O_5 and 4.15 g of dipicolinic acid were dissolved in 100 ml of H_2O at $70^\circ C$. The solution was cooled to room temperature and saturated KCl solution was added until a white precipitate began to form. After cooling to $0^\circ C$ with an ice bath, the solution was filtered, and the white precipitate was washed with ethanol and ether. The powder (3.01 g) was then redissolved in a minimum of water at $50^\circ C$, resulting in a light yellow solution, and cooled slowly to room temperature in order to recrystallize the product. After filtration, the white powder was dried in vacuum. The 1H NMR in D_2O is shown in Figure 4-3.

$[VO(O_2)(PA)(H_2O)_2]$. The picolinic acid complex was prepared by the method in reference 53e, with minor modification. 2.26 g of V_2O_5 and 3.08 g of picolinic acid were dissolved in 10 ml of 30% H_2O_2 , at just below $0^\circ C$. It is important to keep the reaction solution at or below $0^\circ C$ to prevent peroxide decomposition. In this case, the reaction solution was immersed in an ice bath where the water was saturated with NaCl to achieve

lower temperature. The peroxide-vanadium oxide-picolinic acid slurry was stirred continuously for 4 hours. The orange precipitate was filtered and washed twice with 5 ml aliquots of ice-cold water and once with diethyl ether. CAUTION: The reaction described here is prone to cause peroxide decomposition should the temperature rise appreciably above 0°C. This reaction should only be carried out in an open beaker, as peroxide decomposition could lead to explosion in a closed reaction system. The ^1H NMR of this complex is shown in Figure 4-4 and is in agreement with the reported ^1H NMR.^{53e} Elemental analysis calculated for $\text{VC}_8\text{H}_8\text{O}_7\text{N}$: %C = 28.02, %H = 3.10, %N = 5.45. Found: %C = 27.80, %H = 3.07, %N = 5.36.

$[\text{VO}(\text{O}_2)(\text{bipy})_2]\text{ClO}_4$. This complex had been previously synthesized,⁵⁸ however the details of the synthesis were omitted. 1.0 g of V_2O_5 , 5.0 ml of 30% H_2O_2 , 1.5 ml HClO_4 , and 3.5 g of 2,2'-bipyridine were added to 100 ml H_2O and 100 ml CH_3CN and stirred 6 hours at room temperature. The temperature was then increased to 50°C, in order to fully dissolve the product, and the reaction mixture was filtered. The filtrate was allowed to stand in the refrigerator overnight, and deep red crystals of the vanadium peroxo complex were formed. The solution was filtered and the crystals collected and washed three times with ethanol, then twice with diethyl ether. Elemental analysis calculated for $\text{VC}_{20}\text{H}_{16}\text{O}_7\text{N}_2\text{Cl}$: %C = 47.03, %H = 3.16, %N = 10.97. Found: %C = 46.82, %H = 3.16, %N = 10.95.

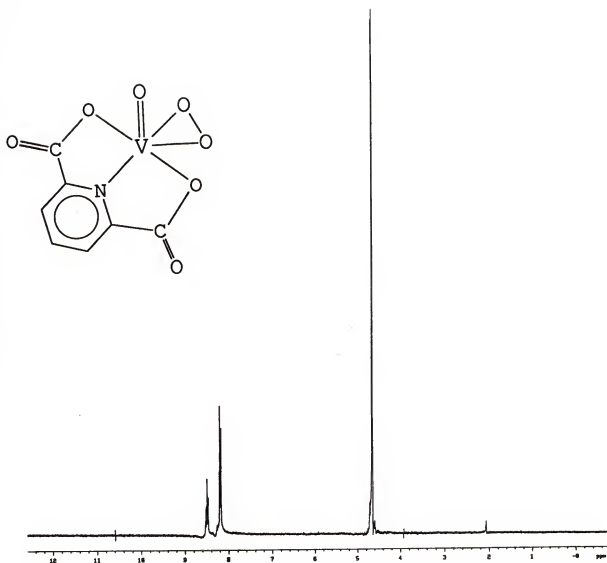


Figure 4-3: 1H NMR of $K[VO_2(dipic)]$. The peaks are at 8.2 (d, 2H) and 8.35 (t, 1H).

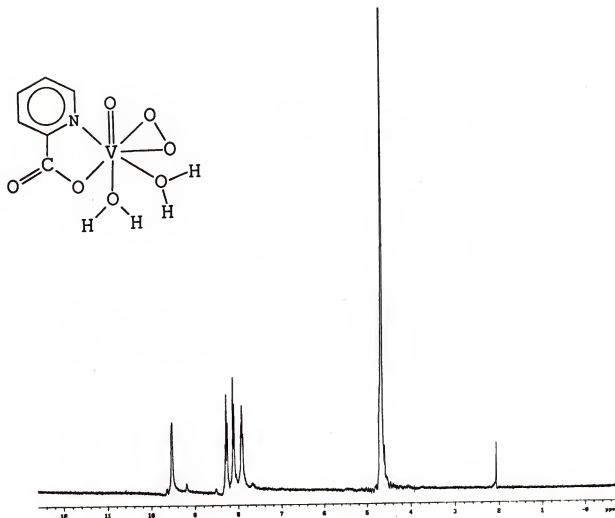


Figure 4-4: ^1H NMR of $[\text{VO}(\text{O}_2)(\text{pic})(\text{H}_2\text{O})_2]$. The peaks are at 7.9 (m, 1H), 8.1 (m, 1H), 8.3 (m, 1H), and 9.5 (s, 1H).

Instrumentation

The concentration of oxidation products as the reaction progressed was measured with a Hewlett-Packard HP5890 II gas chromatograph, equipped with a flame ionization detector. The column used for all separations in this chapter was a HP-50+ capillary column. For cyclohexane oxidations, the products were analyzed with the column temperature at 80°C, giving retention times of 3.85 minutes and 5.11 minutes respectively for cyclohexanol and cyclohexanone. For benzene oxidation, a temperature program was employed with an initial temperature of 90°C and an initial time of 3 minutes, followed by a temperature ramp of 15°C/minute. Under these conditions the phenol retention time is 4.81 minutes.

Procedure For Oxidations

Cyclohexane oxidation: 5 ml of cyclohexane (0.046 moles) and 5 ml of 30% H₂O₂ (0.050 moles) were added to 75 ml CH₃CN, and the solution heated to 50°C. 1.0×10^{-4} moles of catalyst were added to the solution. Small aliquots of the reaction solution were analyzed at regular intervals in order to determine the concentration of the oxidation products.

Benzene oxidation: 5 ml of benzene (0.056 moles) and 5 ml of 30% H₂O₂ (0.050 moles) were added to 75 ml CH₃CN, and the solution heated to 70°C. 3.0×10^{-5} moles of catalyst were added to the solution. Small aliquots of the reaction solution were analyzed at regular intervals to determine the phenol concentration.

Experimental Results And Discussion

Cyclohexane Oxidation

The oxidation of cyclohexane, as catalyzed by certain vanadium complexes, was performed as described above. Four different vanadium complexes were employed as catalysts; $\text{VO}(\text{AcAc})_2$, $\text{VO}(\text{O}_2)(\text{PA})(\text{H}_2\text{O})_2$, $\text{K}[\text{VO}(\text{DPA})]$, and $\text{VO}(\text{O}_2)(\text{bipy})_2$. Figures 4-5, 4-6, and 4-7 show the increase in concentration of cyclohexanol and cyclohexanone for the catalytic oxidation of cyclohexane by each of these complexes. Table 4-1 shows the final yield of products. Peroxide efficiency is calculated by determining the number of oxidizing equivalents used productively per total equivalents of peroxide added. Percent conversion is the fraction of the substrate which was oxidized to cyclohexanol or cyclohexanone.

The vanadium-DPA complex was found to be inactive, and no significant amount of product was observed. This was not surprising, as vanadium complexes formed in situ with tridentate ligands were previously found to be inactive.⁵⁷ As can be seen from Figures 4-6 and 4-7, the vanadium complexes of picolinic acid and bipyridine are all almost identical in their reactivity. This result directly contradicts our predictions about the reactivity of these complexes. With a stronger O-O peroxide bond, and a lower reduction potential, the vanadium-bipy complex should have been much more active, assuming one of the mechanisms in Figure 4-2 apply. The vanadium-AcAc complex is less active than the bipy or PA complexes for catalysis under these conditions (Figure 4-5).

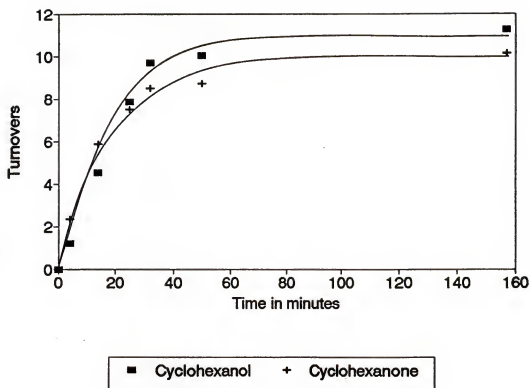


Figure 4-5: Oxidation of cyclohexane catalyzed by the $\text{VO}(\text{AcAc})_2$ complex at 50°C .
 $[\text{C}_6\text{H}_{12}] = 0.046 \text{ M}$, $[\text{H}_2\text{O}_2] = 0.050 \text{ M}$, $[\text{VO}(\text{AcAc})_2] = 1.0 \times 10^{-4} \text{ M}$.

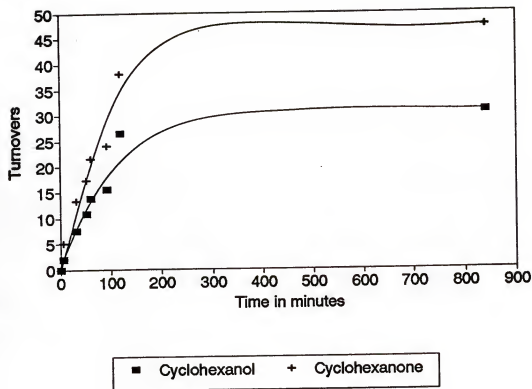


Figure 4-6: Oxidation of cyclohexane catalyzed by the $\text{VO}(\text{O}_2)(\text{bipy})_2$ complex at 50°C . $[\text{C}_6\text{H}_{12}]=0.046\text{ M}$, $[\text{H}_2\text{O}_2]=0.050\text{ M}$, $[\text{VO}(\text{O}_2)(\text{bipy})_2]=1.0 \times 10^{-4}\text{ M}$.

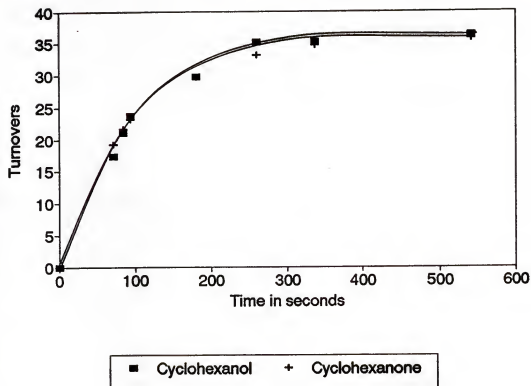


Figure 4-7: Oxidation of cyclohexane catalyzed by the $\text{VO}(\text{O}_2)(\text{pic})(\text{H}_2\text{O})_2$ complex at 50°C . $[\text{C}_6\text{H}_{12}] = 0.046 \text{ M}$, $[\text{H}_2\text{O}_2] = 0.050 \text{ M}$, $[\text{VO}(\text{O}_2)(\text{pic})(\text{H}_2\text{O})_2] = 1.0 \times 10^{-4} \text{ M}$.

Benzene Oxidation

Three vanadium complexes were examined as potential oxidation catalysts for benzene hydroxylation to phenol. The complexes studied were; $\text{VO}(\text{AcAc})$, $\text{VO}(\text{O}_2)(\text{PA})(\text{H}_2\text{O})_2$, and $\text{VO}(\text{O}_2)(\text{bipy})_2$. Figure 4-8 shows the increase in phenol concentration with time for catalysis by these complexes. The final phenol conversion is shown in Table 4-2. As can be seen from both the graphs and Table 4-2, the overall conversion of benzene to phenol is fairly low. The vanadium-PA and vanadium-bipy complexes both give essentially identical activity, and the vanadium-AcAc complex shows much less activity. These experiments show that the vanadium-bipy complex is not any better than the vanadium-PA complex as a catalyst for benzene oxidation. This is again contrary to our expectations, as we had expected that the vanadium-bipy complex would be greatly superior to the vanadium-PA complex as a catalyst. We are forced to conclude that we can observe no correlation of O-O bond length/strength and catalytic activity in these complexes.

In addition, the peroxide efficiency was very low for our experiments. In the case of benzene hydroxylation to phenol, yield (based on peroxide) was only 3-6%. For the cyclohexane oxidations, the best yield was only 25%. Yields such as this are indicative of direct activation through peroxide decomposition. This may be the reason why the effect of the O-O bond strength on the reactivity was negligible for these complexes, as the primary route for oxidation was through decomposition rather than through oxygen atom transfer from the vanadium complex. These low yields demonstrate that even when a decomposition-free pathway exists, peroxide

Table 4-1: Conversion and efficiency of the vanadium catalysts studied for cyclohexane oxidation.

Catalyst	$C_6H_{11}OH^a$	$C_6H_{10}O^a$	% Conversion ^b	% Efficiency ^c
$VO(O_2)(PA)(H_2O)_2$	0.043	0.042	15%	22%
$VO(O_2)(bipy)_2$	0.036	0.056	17%	25%
$VO(AcAc)_2$	0.022	0.012	6%	5%
$K[VO(DPA)]$	0.0	0.0	0%	0%

^a Products are expressed as moles/liter

^b Percent conversion is the fraction of cyclohexane converted to cyclohexanone and cyclohexanol.

^c Peroxide efficiency is based on the number of moles peroxide used productively per total mole of peroxide.

Table 4-2: Effectiveness and efficiency of the vanadium catalysts for benzene oxidation.

Catalyst	$[C_6H_5OH]^a$	% Conversion ^b	% Efficiency ^c
$VO(O_2)(PA)(H_2O)_2$	0.036	6%	6%
$VO(O_2)(bipy)_2$	0.036	6%	6%
$VO(AcAc)_2$	0.015	2%	2%

^a Products are expressed as moles/liter

^b Percent conversion is the fraction of benzene converted to phenol.

^c Peroxide efficiency is based on the number of moles peroxide used productively per total mole of peroxide.

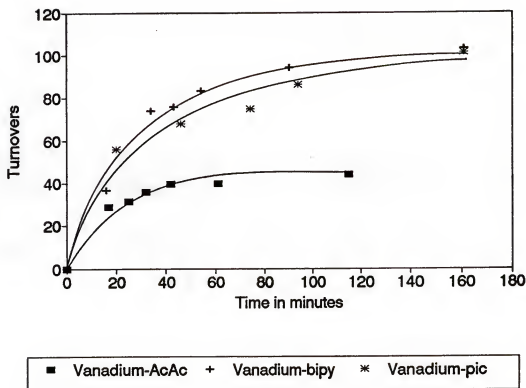


Figure 4-8: Oxidation of benzene to phenol catalyzed by vanadium complexes
 $[\text{H}_2\text{O}_2] = 0.050 \text{ M}$, $[\text{C}_6\text{H}_6] = 0.056$, $[\text{catalyst}] = 3.0 \times 10^{-3} \text{ M}$.
 This reaction was carried out at 70°C .

decomposition pathways may compete with the productive oxidation pathways to give poor efficiency.

Conclusion

As discussed in the introduction, it was anticipated that a vanadium complex with an unusually short O-O peroxide bond length might give superior activity for catalytic oxidation. The effect of the O-O bond strength on the reactivity of peroxo complexes was investigated in the mid-1970's by Vaska,⁶¹ and as a rule, no correlation exists between O-O bond strength and reactivity. However, given the necessity for electron transfer to the vanadium in the reaction mechanisms shown previously, and the dependence of the reduction potential on O-O bond strength,⁵⁶ it was thought vanadium complexes might be an exception to that rule.

The lack of a significant difference in reactivity between the vanadium-PA and vanadium-bipy complexes illustrates there is, in fact, no exception to the rule here. This is despite a very large difference in the O-O bond length in these complexes. The vanadium-bipy O-O peroxo bond length is 1.24 Å,⁵⁸ while the O-O bond length for the vanadium-PA complex is 1.44 Å.^{53c} In addition, for the oxidation of benzene most of the peroxide was lost to decomposition. This is not totally unexpected, as radical pathways, which can lead to radical chain decomposition, dominate the mechanisms for oxidation by these complexes. The yields based on peroxide can be increased by using a great excess of substrate, or by adding the peroxide in small aliquots to ensure that at any given time the concentration of substrate is much greater than the concentration of the peroxide.^{54c,e}

However, the low yields based on peroxide achieved in these experiments show that under our conditions, the pathway leading to decomposition dominates.

CHAPTER 5 CONCLUSION

In our investigation of the activation of hydrogen peroxide, we found that the single factor which most dominates this type of catalysis is peroxide decomposition. The use of peroxide in an effective and efficient way is greatly hampered by this problem. Chapter 2 presents a method for predicting the conditions under which peroxide decomposition is catalyzed. For transition metal complexes which activate hydrogen peroxide through a two-electron transfer pathway (as occurs with a Class III mechanism), only complexes with two-electron reduction potentials sufficiently low to preclude peroxide oxidation will be efficient peroxide activators.

In chapter 3, a series of copper(II) complexes were examined as peroxide activation catalysts in basic aqueous solution. Only copper(II) complexes with two equatorial coordination sites occupied by easily displaced water were found to activate hydrogen peroxide for oxidation. Based on our results, we propose that a copper(II)-hydroperoxide complex is responsible for the oxidation. This conclusion is based on our kinetic studies and the survey of reactivity with different ligands. The only cases where an active catalyst system formed was when the predominant species in solution is the 1:1 bidentate ligand to copper complex. Tri-dentate ligands were found to be much less active, and the binding of two bidentate ligands results in an inactive

complex. The need for two available coordination sites has no viable explanation other than the coordination of peroxide anion to the copper(II) center.

Several vanadium peroxo complexes were also examined. The connection between peroxo O-O bond length and reduction potential seemed to imply that a complex with an unusually short O-O bond length might show greatly superior catalytic activity. This conclusion was based on examination of the mechanisms proposed by Mimoun^{53b} and Di Fulvia^{54b,c}. However, experimental results show that O-O bond length has no real effect on the reactivity of these complexes for oxidative catalysis with peroxide. This is attributed to the domination of radical pathways to substrate oxidation, a Class IVa mechanism, over O-atom transfer to substrate through a Class IVb mechanism. This result emphasizes the importance of avoiding the decomposition pathways, as the availability of this pathway greatly lowers product yields.

LIST OF REFERENCES

- 1) Drago, R. S. *Coord. Chem. Rev.* **1992**, *117*, 185.
- 2) Drago, R. S.; Beer, R. H. *Inorg. Chim. Acta.* **1992**, *198*, 359.
- 3) Drago, R. S.; Corden, B.B. *Acc. Chem. Res.* **1980**, *13*, 353.
- 4) Drago, R. S. *Inorg. Chem.* **1979**, *18*, 1408.
- 5) Drago, R. S.; Beuselsdijk, T.; Breese, J. A.; Cannady, J. P. *J. Am. Chem. Soc.* **1978**, *100*, 5373.
- 6) Drago, R. S.; Cannady, J. P.; Leslie, K. A. *J. Am. Chem. Soc.* **1980**, *102*, 6017.
- 7) Drago, R. S.; Hamilton, D. E.; Telser, J. J. *J. Am. Chem. Soc.* **1984**, *106*, 5353.
- 8) Holm, R. H. *Chem. Rev.* **1987**, *87*, 1401.
- 9) Fenton, H. J. H. *J. Am. Chem. Soc.* **1943**, *65*, 899.
- 10) Saussine, L.; Brazi, E.; Robine, A.; Mimoun, H.; Fischer, J.; Weiss, R. *J. Am. Chem. Soc.* **1985**, *107*, 3534 (and references therein).
- 11) Backvall, J. E.; Akermark, B.; Ljunggren, S. S. *J. Am. Chem. Soc.* **1979**, *101*, 2411.
- 12) Wilson, S. *Chemistry & Industry*, **1994**, 257.
- 13) Comyns, A. E. *Nature* **1994**, *369*, 609.
- 14) Hage, R.; Iburg, J. E.; Kerschner, J.; Koek, J. H.; Lempers, E. L. M.; Martens, R. J.; Racherla, U. S.; Russell, S. W.; Swarthoff, T.; van Vliet, M. R. P.; Warnaar, J. B.; van der Wolf, L.; Krijnen, B. *Nature* **1994**, *369*, 637.
- 15) (a) Che, C. M.; Lai, T. F.; Chan, C. W.; *J. Chem. Soc.* **1994**, 895.
 (b) Che, C. M.; Li, C. K.; Tong, W. F.; Lai, T. F.; *J. Chem. Soc.* **1992**, 816.
 (c) Che, C. M.; Leung, W. H.; Li, C. K.; Poon, C. K.; *J. Chem. Soc.* **1991**, 379.
 (d) Che, C. M.; Wong, K. Y.; Lee, W. O.; *J. Electroanal. Chem.* **1991**, *319*, 207.
 (e) Che, C. M.; Lau, K.; Lau, T. C.; Poon, C. W.; *J. Am. Chem. Soc.* **1990**, *112*, 5176.

- (f) Che, C. M.; Tong, W. T.; Lee, W. O.; Wong, W. T.; Lai, T. F. *J. Chem. Soc.* **1989**, 2011.
 - (g) Che, C. M.; Tang, W. T.; Wong, W. T.; Lai, T. F. *J. Am. Chem. Soc.* **1989**, *111*, 9048.
 - (h) Che, C. -M.; Lee, W. O. *J. Chem. Soc., Chem. Commun.* **1988**, 881.
 - (i) Lau, T. C.; Che, C. M.; Lee, W. O.; Poon, C. K. *J. Chem. Soc., Chem. Commun.* **1988**, 1406.
 - (j) Che, C. M.; Leung, W. H. *J. Chem. Soc., Chem. Commun.* **1987**, 1376 .
 - (k) Che., C. M.; Leung, W. H. ; Poon C. K. *J. Chem. Soc. , Chem. Commun.* **1987**, 173.
 - (l) Che, C. M.; Lai, T. F.; Wong, K. Y. *Inorg. Chem.* **1987**, *26*, 2289.
 - (m) Che, C. M.; Wong, K. Y.; Leung, W. H. ; Poon C. K. *Inorg. Chem.* **1986**, *25*, 345.
- 16) (a) Meyer, T. J.; Dovletoglou, A. *J. Am. Chem. Soc.* **1994**, *116*, 215.
- (b) Meyer, T. J.; Roecker, L. E.; Seok, W. K.; Dovletoglou, A.; McGuire, M. E.; Binstead, R. A. *J. Am. Chem. Soc.* **1992**, *114*, 173.
 - (c) Meyer, T. J. ; Geselowitz, O. *Inorg. Chem.* **1990**, *29*, 3894.
 - (d) Meyer, T. J.; Dovletoglou, A. Adeyemi, S. A.; Lynn, M. H.; Hodgson, D. J. *J. Am. Chem. Soc.* **1990**, *112*, 8989.
 - (e) Meyer, T. J. ; Llobet, A.; Hodgson, D. J. *Inorg. Chem.* **1990**, *29*, 3760.
 - (f) Meyer, T. J.; Dobson, J. C.; Helms, J. H.; Doppelt, P.; Sullivan, B. P.; Hatfield, W. E. *Inorg. Chem.* **1989**, *28*, 2200.
 - (g) Meyer, T. J. ; Dobson, J. C. *Inorg. Chem.* **1988**, *27*, 3283.
 - (h) Meyer, T. J. ; Roecker, L. *J. Am. Chem. Soc.* **1987**, *109*, 746.
 - (i) Meyer, T. J. ; Roecker, L.; Dobson, J. C.; Vining, W. J. *Inorg. Chem.* **1987**, *26*, 779.
 - (j) Meyer, T. J. ; Gilbert, J. Roecker, L. *Inorg. Chem.* **1987**, *26*, 1126.
 - (k) Meyer, T. J. ; Dobson, T. C.; Seok, W. K. *Inorg. Chem.* **1986**, *25*, 1514.
- 17) (a) Takeuchi, K. J. ; Muller, J. G.; Acquaye, J. H. *Inorg. Chem.* **1992**, *31*, 4552.
- (b) Takeuchi, K. J. ;Marmion, M. E. *J. Am. Chem. Soc.* **1988**, *110*, 1472.
 - (c) Takeuchi, K. J. ; Leising , R. A.; Ohman, J. S. *Inorg. Chem.* **1988**, *27*, 3804.
 - (d) Takeuchi, K. J. ; Marmion, M. E. *J. Chem. Soc., Chem. Commun.* **1987**, *108*, 1396.
 - (e) Takeuchi, K. J. ; Marmion, M. E. *J. Am. Chem. Soc.* **1986**, *108*, 510.
- 18) (a) Groves, J. T.; Ahn, K. -H; Quinn, R. *J. Am. Chem. Soc.* **1988**, *110*, 4217.
- (b) Groves, J. T.; Ahn, K. -H. *Inorg. Chem.* **1987**, *26*, 3831.
 - (c) Groves, J. T.; Quinn, R. *J. Am. Chem. Soc.* **1985**, *107*, 5790.
 - (d) Groves, J.T; Quinn, R. *Inorg. Chem.* **1984**, *23*, 3844.

- 19) (a) Drago, R. H.; Beer, R. H.; Goldstein, A. S. *J. Am. Chem. Soc.* **1994**, *116*, 2424
 (b) Goldstein, A. S.; Drago, R. S. *J. Chem. Soc., Chem. Commun.* **1991**, 21.
 (c) Bailey, C. L.; Drago, R. S. *J. Chem. Soc., Chem. Commun.* **1987**, 179.
- 20) Sauvage, J. P.; Collins, J. P. *Inorg. Chem.* **1990**, *29*, 2303.
- 21) Bard, A. J.; Faulkner, L. R. *Electrochemical Methods*, Wiley: New York, **1980**.
- 22) (a) Meyer, T. J.; Takeuchi, K. J.; Thompson, M. S. Pipes, D. W. *Inorg. Chem.* **1984**, *23*, 1845.
 (b) Meyer, T. J.; Moyer, B. A. *Inorg. Chem.* **1981**, *20*, 436.
- 23) Laidler, K. *Chemical Kinetics*, Harper and Row: New York, **1987**.
- 24) Greenwood, N. N.; Earnshaw, A. *Chemistry of the Elements*, Pergamon Press: New York, **1989**.
- 25) Atkins, P. W.; *Physical Chemistry*, W. H. Freeman and Company: New York, **1986**.
- 26) Latimer, W. M. *Oxidation Potentials*; Prentice-Hall: New York, **1952**.
- 27) Sheldon, R. A.; Kochi, J. K. *Metal-Catalyzed Oxidations of Organic Compounds*, Academic Press, New York, **1981**.
- 28) a) Sawyer, D. T.; Cepak, V.; Redman, C.; Kang, C. *Bioorg. & Med. Chem.* **1993**, *1*, 125.
 b) Sawyer, D. T.; Kang, C.; Tung, H. C. *J. Am. Chem. Soc.* **1992**, *114*, 3445.
 c) Sawyer, D. T.; Kanofsky, J. R.; Sobkowiak, A.; Ross, B.; Cofré, P.; Richert, S. A.; Shew, C. *J. Am. Chem. Soc.* **1990**, *112*, 1936.
- 29) a) Barton, D. H. R.; Balavoine, G.; Boivin, J.; Gref, A. *Tetrahedron Lett.* **1990**, *31*, 659.
 b) Barton, D. H. R.; Balavoine, G.; Boivin, J.; Gref, A.; Coupanec, P. L.; Ozbalik, N.; Pestana, J. A. X.; Riviere, H. *Tetrahedron* **1990**, *44*, 1091.
 c) Barton, D. H. R.; Balavoine, G.; Boivin, J.; Gref, A.; Ozbalik, N.; Riviere, H. *Tetrahedron Lett.* **1986**, *27*, 2849.
 d) Barton, D. H. R.; Balavoine, G.; Boivin, J.; Gref, A.; Ozbalik, N.; Riviere, H. *J. Chem. Soc., Chem. Commun.* **1986**, 1727.
 e) Barton, D. H. R.; Boivin, J.; Ozbalik, N.; Schwartzentruber, K. M.; Jankowski, K. *Tetrahedron Lett.* **1985**, *26*, 447.

- 30) a) Ellis, S. R. US Patent 5041142, Aug. 20, 1991.
b) Hage, R.; Favre, T. L. F.; Helm-Rademacher, K.; Koek, H.; Martens, R. J.; Swarthoff, T.; Vliet, M. R. P. European Patent 0458397A2, May, 15, 1991.
c) Hage, R.; Favre, T. L. F.; Helm-Rademacher, K.; Koek, H.; Martens, R. J.; Swarthoff, T.; Vliet, M. R. P. European Patent 0458398A2, May, 15, 1991.
d) Harriot, S. M. US Patent 5021187, Jun. 4, 1991.
e) Bragg, C. D.; Hardy, P. A. US Patent 5002682, Mar. 26, 1991.
f) Dolphin, D. H.; Nakano, T.; Kirk, T. K.; Wijesekera, T. P.; Farrell, R. L.; Maione, T. E. US Patent 5041142, Aug. 20, 1991.
g) Oakes, J. US Patent 4481129, Nov. 6, 1984.
- 31) Kushioka, K.; Tanimoto, I.; Maruyama, K. *Bull Chem. Soc. Jpn.* **1989**, *62*, 1147.
- 32) a) Sawyer, D. T.; Llober, A.; Liu, X.; Qui, A.; Sobkowiak, A. *J. Am. Chem. Soc.* **1993**, *115*, 609.
b) Sawyer, D. T.; Qiu, A.; Liu, X. *J. Am. Chem. Soc.* **1993**, *115*, 3239.
- 33) a) Kitajima, N.; Fujisawa, K.; Fujimoto, C.; Moro-oka, Y.; Hashimoto, S.; Kitagawa, T.; Toriumi, K.; Tatsumi, K.; Nakamura, A. *J. Am. Chem. Soc.* **1992**, *114*, 1277.
b) Kitajima, N.; Koda, T.; Hashimoto, S.; Kitagawa, T.; Moro-oka, Y. *J. Am. Chem. Soc.* **1991**, *113*, 5664.
c) Kitajima, N.; Fujisawa, K.; Moro-oka, Y. *J. Am. Chem. Soc.* **1989**, *111*, 8975.
- 34) Sorrell, T. N.; Garrity, M. L. *Inorg. Chem.* **1991**, *30*, 210.
- 35) a) Karlin, K. D.; Zubieta, J.; Chen, Q.; Murthy, N. N.; Wei, N. *Inorg. Chem.* **1994**, *33*, 1953.
b) Karlin, K. D.; Tyeklár, Z.; Murthy, N. N.; Wei, N. W. *Inorg. Chem.* **1994**, *33*, 1177.
c) Karlin, K. D.; Cohen, B. I.; Nasir, M. S.; *J. Am. Chem. Soc.* **1992**, *114*, 2482.
d) Karlin, K. D.; Solomon, E. I.; Tyeklár, Z.; Pate, J. E.; Ross, P. K.; Baldwin, M. *J. Am. Chem. Soc.* **1991**, *113*, 8671.
e) Karlin, K. D.; Solomon, E. I.; Cruse, R. W.; Pate, J. E. *J. Am. Chem. Soc.* **1987**, *109*, 2624.
- 36) a) Solomon, E. I.; Kitajima, N.; Fujisawa, K.; Pate, J. E.; Root, D. E.; Baldwin, M. *J. Am. Chem. Soc.* **1992**, *114*, 10421.
b) Solomon, E. I.; Ballou, D. P.; Cole, J. L. *J. Am. Chem. Soc.* **1991**, *113*, 8544.

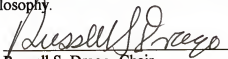
- 37) a) Kitajima, N.; Moro-oka, Y.; Katayama, T.; Fujisawa, K.; Iwata, Y. *J. Am. Chem. Soc.* **1993**, *115*, 7872.
 b) Kitajima, N.; Fujisawa, K.; Moro-oka, Y. *Inorg. Chem.* **1990**, *29*, 357.
- 38) Byers, G. W.; Gross, S.; Henrichs, P. M. *Photochem. Photobiol.* **1976**, *23*, 37.
- 39) a) Espenson, J. H.; Bakac, A.; Janni, J. *J. Am. Chem. Soc.* **1994**, *116*, 3436.
 b) Espenson, J. H.; Bakac, A.; Chen, W. J.; Scott, S. L. *J. Phys. Chem.* **1993**, *97*, 6710.
- 40) a) Bruice, T. C.; Smith, J. R. L.; Balasubramanian, P. N. *J. Am. Chem. Soc.* **1988**, *110*, 7411.
 b) Bruice, T. C.; Schmidt, E. S.; Balasubramanian, P. *J. Am. Chem. Soc.* **1987**, *109*, 7865.
 c) Bruice, T. C.; Zippies, M. F.; Lee, W. A. *J. Am. Chem. Soc.* **1986**, *108*, 4433.
- 41) Werner, W.; Wielinger, H.; Gawehn, K. *Z. Anal. Chem.* **1970**, *252*, 222.
- 42) Bardsley, W. G.; Childs, R. E. *Biochem. J.* **1975**, *145*, 93.
- 43) Sayre, L. M.; Wang, F. *Inorg. Chem.* **1989**, *28*, 169.
- 44) Saltman, P.; Hegetschweiler, K. *Inorg. Chem.* **1986**, *25*, 107.
- 45) Smith, R. M.; Martell, A. E. *Critical Stability Constants, Vol. 1-3*, Plenum Press, New York, **1975**.
- 46) van Eldik, R.; Meyerstein, D.; Cohen, H.; Czapski, G.; Goldstein, S. *Inorg. Chem.* **1994**, *33*, 3255.
- 47) Margerum, D. W.; Scheper, W. M.; McDonald, M. R.; Fredericks, F. C.; Wang, L.; Lee, H. D. In *Bioinorganic Chemistry of Copper*, Karlin, K. D., Tyeklár, Z. Eds, Chapman and Hall, New York, **1993**.
- 48) Di Furia, F.; Conte, V. In *Catalytic Oxidations with Hydrogen Peroxide as Oxidant*, Strukul, G. Ed., Kluwer Academic Publishers, Boston, **1992**.
- 49) Mimoun, H. In *Comprehensive Coordination Chemistry, Vol. 6*, Wilkinson, G. Ed., Pergamon Press, New York, **1987**.
- 50) Armstrong, F. B. *Biochemistry*, Oxford University Press, New York, **1989**.
- 51) Di Furia, F.; Conte, V.; Modena, G. In *Organic Peroxides*, Ando, W. Ed., Wiley, New York, **1992**.

- 52) Di Furia, F.; Modena, G.; Conte, V.; Bonchio, M.; Coppa, F. In *Dioxygen Activation and Homogeneous Catalytic Oxidations*, Simandi, L. I., Ed., Elsevier, Amsterdam, **1991**.
- 53) a) Mimoun, H.; Mignard, M.; Brechot, P.; Saussine, L. *J. Am. Chem. Soc.* **1986**, *108*, 3711.
b) Mimoun, H.; Saussine, L.; Daire, E.; Postel, M.; Fischer, J.; Weiss, R. *J. Am. Chem. Soc.*, **1983**, *105*, 3101.
c) Mimoun, H.; Chaumette, P.; Mignard, M.; Saussine, L. *Nouv. J. Chim.* **1983**, *7*, 467.
- 54) a) Modena, G.; Di Furia, F.; Moro, S.; Conte, V.; Bonchio, M. *Inorg. Chem.* **1994**, *33*, 1631.
b) Modena, G.; Di Furia, F.; Conte, V.; Bonchio, M.; Moro, S. *J. Org. Chem.* **1994**, *59*, 6262.
c) Modena, G.; Di Furia, F.; Moro, S.; Standen, S.; Conte, V.; Coppa, F.; Bonchio, M.; Bianchi, M. *J. Mol. Catal.* **1993**, *83*, 107.
d) Di Furia, F.; Conte, V.; Toscano, R. M.; Tomaselli, G. A.; Ballistrei, F. P. *J. Am. Chem. Soc.* **1991**, *113*, 6209.
e) Modena, G.; Di Furia, F.; Conte, V.; Bonchio, M. *J. Org. Chem.* **1989**, *54*, 4368.
f) Modena, G.; Di Furia, F.; Conte, V. *J. Org. Chem.* **1988**, *53*, 1665.
- 55) Zamarayev, K. I.; Babenko, V. P.; Chinakov, V. D.; Talsi, E. P. *J. Mol. Catal.* **1993**, *81*, 235.
- 56) Modena, G.; Di Furia, F.; Conte, V.; Bonchio, M.; Moro, S.; Pastore, P.; Magno, F.; Carofiglio, T. *Inorg. Chem.* **1993**, *22*, 5797.
- 57) Shul'pin, G. B.; Attanasio, D.; Suber, L. *J. Catal.*, **1993**, *142*, 147.
- 58) Sergienki, V. S.; Borzunov, V. K.; Porai-Koshits, M. A.; Loginov, S. V. *Zh. Neorg. Khim.* **1988**, *33*, 1609.
- 59) Wieghardt, K. *Inorg. Chem.* **1978**, *16*, 57.
- 60) Schwendt, P.; Sivak, M.; Shepelev, Y. F.; Smolin, Y. I.; Lapshin, A. E.; Gyepesova, D. *Trans. Met. Chem.* **1994**, *19*, 34.
- 61) Vaska, L. *Acc. Chem. Res.* **1976**, *9*, 175.

BIOGRAPHICAL SKETCH

Michael Howland Robbins was born in Plattsburgh, NY, on October 11, 1968, and grew up in the Champlain Valley of New York state. He earned a B.S. in Chemistry degree from the State University of New York at Plattsburgh in 1990, doing his undergraduate research with Dr. Gerald Kokoszka. After graduation, having had enough of the cold upstate New York winters, the author moved to Gainesville to continue his education at the University of Florida. In 1990, he joined the Drago group at the University of Florida to work towards a Ph.D. degree in inorganic chemistry. After graduation, Michael Robbins will began work at The Clorox Company in Pleasanton, California, and continue to avoid the cold winters.

I certify that I have read this study and that in my opinion it conforms to acceptable standards of scholarly presentation and is fully adequate, in scope and quality, as a dissertation for the degree of Doctor of Philosophy.



Russell S. Drago, Chair
Graduate Research Professor of
Chemistry

I certify that I have read this study and that in my opinion it conforms to acceptable standards of scholarly presentation and is fully adequate, in scope and quality, as a dissertation for the degree of Doctor of Philosophy.



James Boncella
Associate Professor of Chemistry

I certify that I have read this study and that in my opinion it conforms to acceptable standards of scholarly presentation and is fully adequate, in scope and quality, as a dissertation for the degree of Doctor of Philosophy.



Daniel Talham
Assistant Professor of Chemistry

I certify that I have read this study and that in my opinion it conforms to acceptable standards of scholarly presentation and is fully adequate, in scope and quality, as a dissertation for the degree of Doctor of Philosophy.



Martin Vala
Professor of Chemistry

I certify that I have read this study and that in my opinion it conforms to acceptable standards of scholarly presentation and is fully adequate, in scope and quality, as a dissertation for the degree of Doctor of Philosophy.



Saundra Tenbroeck
Associate Professor of Animal
Science

This dissertation was submitted to the Graduate Faculty of the Department of Chemistry in the College of Liberal Arts and Sciences and to the Graduate School and was accepted as partial fulfillment of the requirements for the degree of Doctor of Philosophy.

May, 1995

Dean, Graduate School